

Discovery of Substituted Di(pyridin-2-yl)-1,2,4-thiadiazol-5-amines as Novel Macroparasiticidal Compounds for the Treatment of Human Filarial Infections

Natalie Hawryluk,* Dale Robinson, Yixing Shen, Graham Kyne, Matthew Bedore, Sanjay Menon, Stacie Canan, Thomas von Geldern, Simon Townson, Suzanne Gokool, Alexandra Ehrens, Marianne Koschel, Nathaly Lhermitte-Vallarino, Coralie Martin, Achim Hoerauf, Geraldine Hernandez, Deepak Dalvie, Sabine Specht, Marc Peter Hübner, and Ivan Scandale



Cite This: *J. Med. Chem.* 2022, 65, 11388–11403



Read Online

ACCESS |



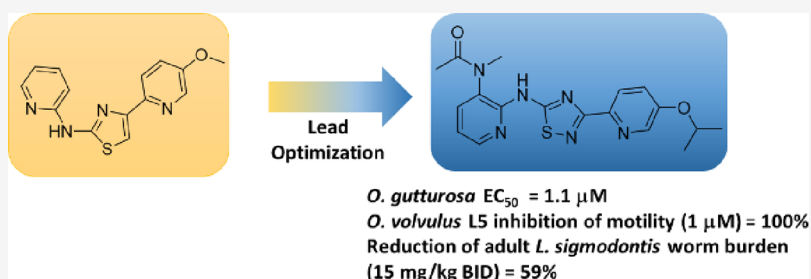
Metrics & More



Article Recommendations



Supporting Information



ABSTRACT: Filarial diseases, including lymphatic filariasis and onchocerciasis, are considered among the most devastating of all tropical diseases, affecting about 145 million people worldwide. Efforts to control and eliminate onchocerciasis are impeded by a lack of effective treatments that target the adult filarial stage. Herein, we describe the discovery of a series of substituted di(pyridin-2-yl)-1,2,4-thiadiazol-5-amines as novel macrofilaricides for the treatment of human filarial infections.

INTRODUCTION

Onchocerciasis and lymphatic filariasis (LF) affect an estimated 145 million people worldwide, creating a serious health burden in endemic areas such as sub-Saharan Africa and India. Filarial nematodes are the pathogens responsible for a number of parasitic diseases; *Onchocerca volvulus* causes onchocerciasis (river blindness), and *Wuchereria bancrofti*, *Brugia malayi*, and *Brugia timori* cause LF (elephantiasis).¹ Current therapies target the juvenile worms (microfilariae), allowing adult worms to continue producing microfilariae. These treatments only temporarily stop transmission, thereby requiring repeat treatments for up to 15 years, depending on the disease.² The need for repeated drug administration, concerns about serious *Loa loa*-related adverse events,³ and the possible emergence of ivermectin-resistant *O. volvulus* have heightened the need for compounds that exhibit adult stage selectivity (macrofilaricidal) or long-lasting sterilizing effects.⁴

Current efforts to control and eliminate onchocerciasis are hindered by the lack of medicines that target the adult worm stage.² In addition, a major challenge hampering drug discovery is finding suitable preclinical animal models as *O. volvulus* can only develop fully in humans and primates. While assays for testing against *O. volvulus* have been established, they have limitations. The use of surrogate parasites is required for

both *ex vivo* and *in vivo* evaluation due to limited accessibility of the adult stage of *O. volvulus*.⁵ Widely used surrogate parasites include the bovine filariae *Onchocerca gutturosa* and *Litomosoides sigmodontis* as the most suitable sources of viable adult filariae for high-throughput screening.⁶ *L. sigmodontis*, a natural filarial parasite of rodents, has been used as a standard model to validate macrofilaricidal drug candidates in a consortium led by the Bill & Melinda Gates Foundation, Drugs for Neglected Diseases initiative (DNDi), academia, and pharmaceutical companies and has supported the advancement of a few macrofilaricidal candidates through preclinical and clinical development.^{7–14}

We recently reported a platform utilizing surrogate nematodes in phenotypic *ex vivo* assays to assess activity across various parasites for the identification of potential novel macrofilaricidal compounds for further drug discovery lead optimization efforts. These efforts led to a series of amino-

Received: June 17, 2022

Published: August 16, 2022



thiazole molecules demonstrating *ex vivo* killing of adult *O. gutturosa*, *B. malayi*, *B. pahangi*, and *L. sigmodontis*.¹⁵ Compound **1** (Figure 1) showed a significant 68% reduction

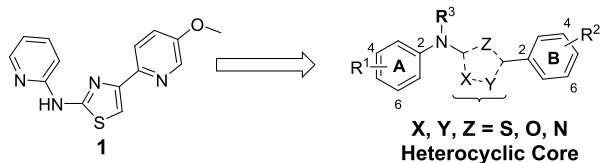


Figure 1. Initial amino thiazole hit molecule, **1**, and lead optimization progression to a novel scaffold.

of adult *L. sigmodontis* worms in infected mice, thus establishing proof of principle for this series and suggesting the potential for further optimization. Herein, we describe the discovery of a series of substituted di(pyridin-2-yl)-1,2,4-thiadiazol-5-amines as novel macrofilaricides for the treatment of onchocerciasis.

As part of our lead optimization efforts, our initial focus was replacement of the thiazole ring core to address potential metabolic instability promiscuity and/or metabolism to a reactive species.^{16–18}

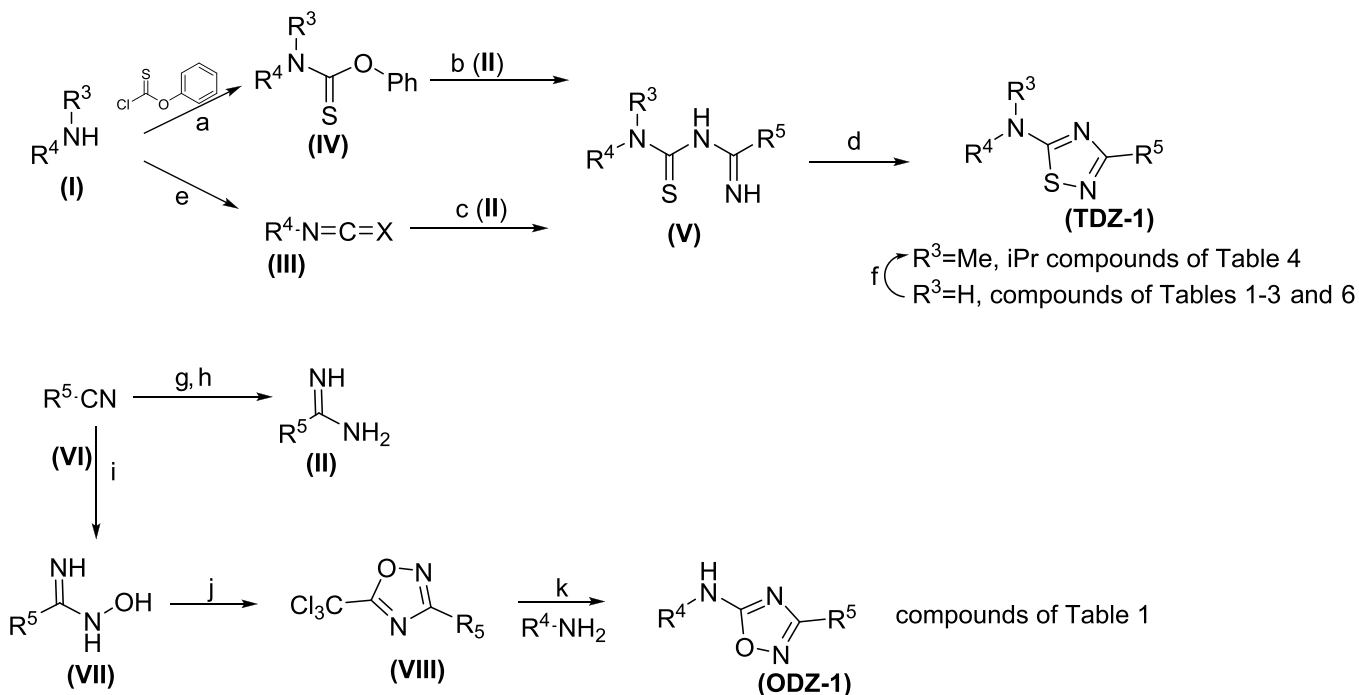
Compound **1** showed sufficient plasma exposure in male CD-1 mice when dosed orally (30 mg/kg); however, dosing was required three times per day (TID) to achieve plasma drug concentrations that would remain continuously above EC₅₀ for 24 h. Although multiple compounds in the amino thiazole (AT) series had reasonable S9 stability, plasma exposure could not be maintained for 24 h. This could be explained by reported metabolism of thiazole moieties.^{18,19}

CHEMISTRY

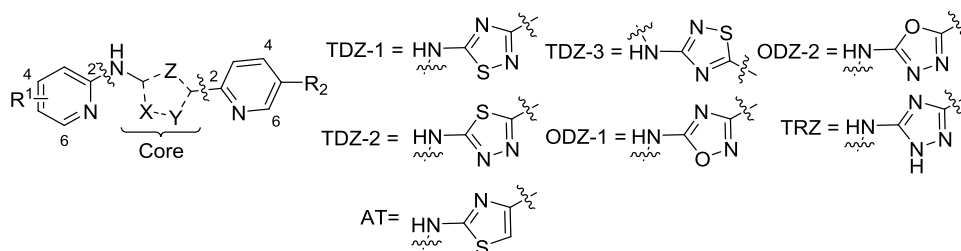
Compounds containing the 1,2,4-thiadiazole core (TDZ-1) are synthesized via a convergent synthesis outlined in Scheme 1. Compounds in Tables 1–3 and 6 are formed by cyclization of (V), which is formed by the addition of an amidine (II) with an isothiocyanate (III). Isothiocyanate (III) can be obtained by reaction of commercially available amines with thiophosgene. Amidine (II) is formed by a Pinner reaction of an appropriately substituted nitrile (VI). Compounds in Table 4 are formed by either direct alkylation of (TDZ-1) or by addition of carbamothioate (IV) to amidine (II) to form (V). Compounds containing the 1,2,4-oxadiazole core (ODZ-1) are synthesized, as described in Scheme 1. Compounds in Table 1 are prepared by the cyclocondensation of amidine oxime (VII) and trichloroacetic anhydride. Amidine oxime (VII) is formed from the corresponding nitrile (VI), and the introduction of the B-ring is achieved via S_NAr chemistry with the analogous amine.

Compounds containing the 1,3,4-thia (TDZ-2) and oxadiazole core (ODZ-2) in Table 1 are prepared by either dehydrative or desulfurative cyclization of thiosemicarbazide (XII) (Scheme 2). The thiosemicarbazide (XII) is formed by reacting the isothiocyanate (III) with hydrazide (X), which is prepared from commercially available carboxylic acid (IX). To obtain the 1,3,4-thiadiazole (TDZ-2), thiosemicarbazide (XII) is treated with tosic acid, whereas for the formation of the 1,3,4-oxadiazole (ODZ-2), 1-ethyl-3-(3-dimethylamino-propyl)-carbodiimide (EDCI) is used.²⁰ Alternatively, formation of the 1,3,4-oxadiazole can be accomplished via oxidative desulfurization using *o*-iodoxybenzoic acid (IBX).²¹ Analogs containing the 1,2,4-triazole core (TRZ) in Table 1

Scheme 1. Synthesis of Di(pyridin-2-yl)-1,2,4-thia-diazol-5-amine and Di(pyridin-2-yl)-1,2,4-oxa-diazol-5-amine^a



^aReagents and conditions: (a) K₂CO₃, THF, 0–25 °C, 16 h, 70–92%, (b) (II), DMSO, KOtBu, 25 °C, 16 h 12–72%, (c) Et₃N, DCM/acetone, 15 °C, 2 h, 17–49%, (d) I₂, H₂O₂, EtOH, 25 °C, 1 h, 14–70%, (e) thiophosgene, DCM, 0 °C, 1 h, 66%, (f) MeI or *i*Pr-I, *n*BuLi, THF, –70 °C, 1–16 h, 31–75% (g) NaOMe, MeOH, 15 °C, 14 h, (h) NH₄Cl, 70 °C, 2 h (39–93% for panels (g, h)), (i) NH₂OH HCl, Et₃NH₂, EtOH, 80 °C, 16 h, (j) (Cl₃CO)₂O, toluene, 110 °C, 16 h. (65–97% for panels (i, j)), (k) NaH, THF, 25 °C, 30 min, 12–25%.

Table 1. *Ex Vivo O. gutturosa* Activity across Heterocyclic Core Variants

Analog	R ¹	Core	R ²	<i>O. gutturosa</i> EC ₅₀ μM (SD ^a)	Kinetic solubility (μM) ^b	Rat S9 metabolic stability ^c	Rat Microsomes ^d	Human S9 metabolic stability ^c	Human Microsomes ^d
1	5-OMe	AT	H	0.27 (0.0)	NA ^e	51		59	
2		TDZ-1		1.70 (0.84)	62.70		78		90
3	3-Me	TDZ-1		0.03 (0.71)	7.30	82		84	-
4		TDZ-2		2.6 (0.43)	0.40		89		100
5		TDZ-3		NA ^f	182.00		89		77
6		ODZ-1		0.07 (0.71)	57.50	85		98	
7		ODZ-2		0.94 (0.25)	12.80		39		83
8		TRZ		0.01 (0.35)	201.70		70 (m) ^g		92

^aStandard deviation. ^bThe standard kinetic solubility assay runs on 200 mM concentration range using 10 mM DMSO stock solutions. ^cLiver S9 metabolic stability assay at 3 μM, % remaining @ 60 min. ^dLiver microsome metabolic stability assay at 3 μM, % remaining measured @ 30 min. ^eTested in the mouse not rat. ^fNA = not available due to COVID; however, **5** demonstrated 25% reduction of *L. sigmodontis* adult worm motility at 100 nM.

are synthesized by cyclocondensation of carbamimidothioate (XI) and hydrazide (X). Hydrazide (X) is prepared by esterification of carboxylic acid (IX) with SOCl₂ and subsequent treatment with hydrazine hydrate.

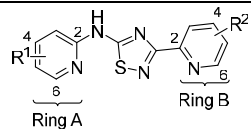

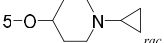
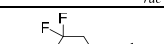
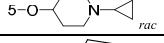
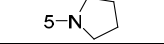
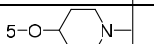
RESULTS AND DISCUSSION

To alleviate the known bioactivation pathway at the C-5 position of the thiazole, we explored a variety of thiadiazoles, oxadiazoles, and triazoles. It had been shown that a number of heteroatoms in a ring, along with their position, have a major role in the metabolism of the heterocyclic ring systems.²²

The 1,2,4-thiadiazoles **2** and **3** maintained good activity as shown by reduction of *O. gutturosa* adult worm motility, whereas the 1,3,4-isomer, (**4**), was less potent by comparison. Overall, all thiadiazole isomers (**3**, **4**, and **5**) showed good metabolic stability (Table 1). A similar trend was observed for the oxadiazole cores (**6** and **7**) that showed good *ex vivo* activity and microsomal stability compared to the aminothiazoles. Both the thiadiazole core (**5**) and the triazole core (**8**) showed improved solubility when compared to the other heterocycles. Additionally, 1,2,4-thiadiazole analog (**2**) of the initial proof of concept compound (**1**) had improved pharmacokinetics (PK) (Table 5) and, although less potent, still demonstrated 50% reduction of adult worm burden *in vivo* (Figure 2A). Based on the consistency of activity²³ and good preliminary PK and demonstration of *in vivo* efficacy, the 1,2,4-thiadiazole core (TDZ-1) was chosen as the primary focus for further exploration.

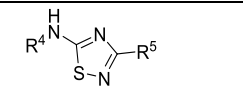
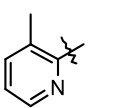
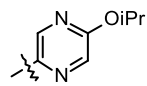
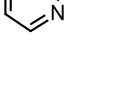
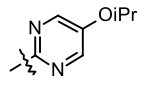
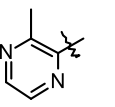
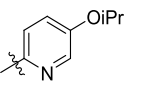
Having identified a replacement for the thiazole core, incorporation of appropriate substituents to achieve optimal physical, chemical, and pharmacokinetic properties was the next goal. SAR quickly revealed that the combination of small alkyl substituents (R¹) on the A-ring, preferably in the 3-position, along with alkoxy groups (R²) in the 5-position of the B-ring showed a marked effect on inhibition of *O. gutturosa* adult worm motility (Table 2) and viability (data in the Supporting Information) while maintaining moderate solubility (10–50 μM) and good metabolic stability (rat and human liver S9 stability of ≥70% remaining at 60 min)²⁴ (Table 2). While many of the new analogs containing the 1,2,4-thiadiazole core demonstrated sub-micromolar inhibition of *O. gutturosa* adult worm motility, the most potent compounds that exhibited *O. gutturosa*, EC₅₀ < 100 nM, contained either a CH₃, *i*Pr, or CF₃ in the 3-position (R¹) and an ether in the 5-position (R²) (i.e., **3**, **10**, **21**, **23**, **24**, and **27**). Incorporation of polarity into the B-ring was generally not detrimental, with some exceptions such as nitrile (**13**) and certain amides (**16**) showing loss of activity. However, combining the nitrile or amide with *O**i*Pr (R²) on the B-ring (**15** and **17**) recovered some of the activity. Introduction of basic amines such as alkylated piperidines as either R¹ or R² improved both aqueous solubility (>10 μM) and metabolic stability while maintaining good activity. Unfortunately, the basic amine imparted a hERG (human ether-a-go-go-related gene) liability (**12** and **19**: hERG IC₅₀ = 0.203 and 3.46 μM, respectively). Interestingly, the reported strategy of substituting piperidines with fluorine atoms to improve metabolism did not prove to be fruitful in

Table 2. *Ex Vivo O. gutturosa* Activity

Analog			<i>O. gutturosa</i> EC ₅₀ μM (SD ^a)	logD ^b	Kinetic solubility μM ^c	Rat S9 metabolic stability ^d	Rat Microso mes ^e	Human S9 metabolic stability ^d	Human Microsom es ^e
	R ¹	R ²							
9	H	H	0.16 (0.35)	1.80	8.20	83		83	
10	3-Me	5-O <i>i</i> Pr	0.06 (0.00)	2.88	3.20	100		100	
11		5-OCyPr	0.11 (0.91)	3.40	1.84	61		76	
12			0.39 (0.41)	2.10	13.08	53		58	
13		5-CN	5.80 (0.35)	2.75	0.55	73		66	
14		4-CN	3.10 (0.35)	2.00	2.55	78		65	
15		4-CN, 5-O <i>i</i> Pr	1.37 (0.87)	2.30	0.30	84		100	
16		4-CO ₂ NMe ₂	3.28 (0.35)	1.90	26.50	78		89	
17		4-CO ₂ NMe ₂ , 5-O <i>i</i> Pr	0.63 (0.35)	2.30	154.50	90		91	
18		5-CO ₂ NMe ₂	0.06 (0.87)	1.70	73.20	94		97	
19			0.06 (1.32)	3.30	3.05	76		83	
20			0.24 (0.50)	2.80	NC ^e	32		52	
21			0.04 (0.35)	2.65	2.17	61		86	
22			0.20 (0.35)	2.00	184.20	81		78	
23	3- <i>i</i> Pr	5-OCyPr	0.04 (0.96)	2.50	0.20	78		39	
24		4-CF ₃ , 5-O <i>i</i> Pr	0.05 (0.55)	2.90	1.05	96		97	
25		5-O <i>i</i> Pr	0.10 (0.87)	2.85	2.58	82		99	
26	3-CF ₃	4-Me	0.03 (0.35)	2.45	0.90	61		56	
27		4- <i>i</i> Pr	0.01 (0.41)	2.50	1.60	27		45	
28	3-OMe	5-O <i>i</i> Pr	0.08 (0.29)	1.70	7.25	100		100	
29		4-Me	0.12 (0.35)	2.10	26.50	70		72	
30	3-NHMe	5-O <i>i</i> Pr	0.22 (1.00)	2.90	1.90	73		86	
31	3-NMe ₂	5-O <i>i</i> Pr	0.08 (0.61)	3.23	22.50	79		86	
32		5-OCyPr	0.74 (0.50)	2.50	8.92	91		100	
33		4-O <i>i</i> Pr, 5-CF ₃	0.85 (0.00)	3.00	1.43	8		100	
34		4-CF ₃ , 5-O <i>i</i> Pr	0.04 (1.19)	2.90	0.00	93		98	
35	4-CF ₃	4- <i>i</i> Pr	0.05 (1.04)	3.0	0.00	45		65	
36		H	1.12 (0.00)	1.70	193.40	99		88	
37	4-CF ₃ , 5- <i>i</i> Pr	5-O <i>i</i> Pr	0.05 (1.06)	2.80	1.00	100		100	
38		3-OCyPr	0.02 (0.00)	2.95	1.03	93		100	

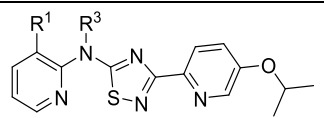
^aStandard deviation. ^bThe log *D* assay runs on 1 M concentration range using 10 mM DMSO stock solutions measured at pH 7.4. ^cThe standard kinetic solubility assay runs on 200 mM concentration range using 10 mM DMSO stock solutions. ^dThe liver S9 metabolic stability assay at 3 μM, % remaining @ 60 min. ^eTested in the mouse and human liver microsomes metabolic stability assay at 3 μM, % remaining measured @ 30 min. ^fNC = not calculated.

Table 3. *Ex Vivo O. gutturosa* Activity with A- and B-Ring Heterocyclic Replacements

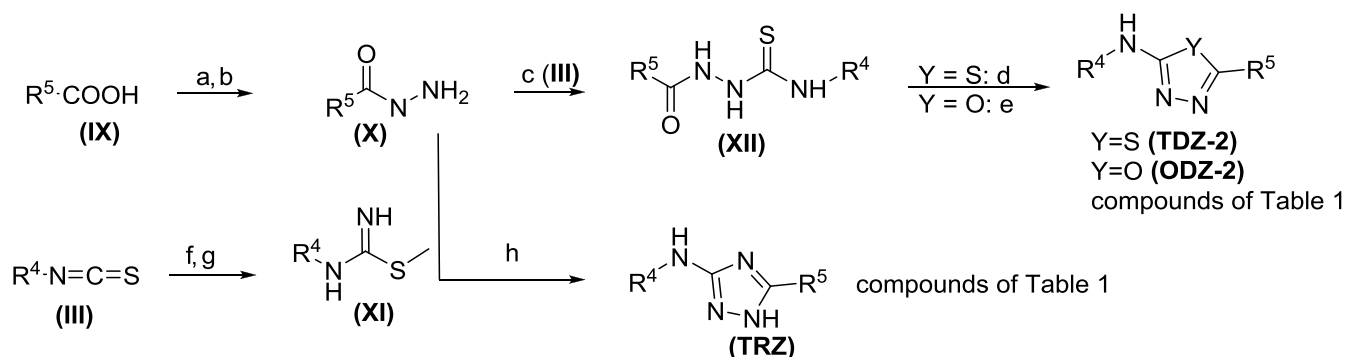
Analog			<i>O. gutturosa</i> EC ₅₀ μM (SD ^a)	logD ^b	Kinetic solubility μM ^c	Rat S9 metabolic stability ^d	Rat Microso mes ^e	Human S9 metabolic stability ^d	Human Microso mes ^e
	R ⁴	R ⁵							
39			0.29 (0.79)	3.10	2.10	74		81	
40			2.35 (0.61)	2.90	12.30		90 ^e		96 ^e
41			0.06 (0.87)	2.70	24.48	100		94	

^aStandard deviation. ^bThe log *D* assay runs on 1 M concentration range using 10 mM DMSO stock solutions measured at pH 7.4. ^cThe standard kinetic solubility assay runs on 200 mM concentration range using 10 mM DMSO stock solutions. ^dLiver S9 metabolic stability assay at 3 μM, % remaining @ 60 min. ^eTested in the mouse and human liver microsome metabolic stability assay at 3 μM, % remaining measured @ 30 min.

Table 4. *Ex Vivo O. gutturosa* Activity Addition of the R³ Substituent

Analog			<i>O. gutturosa</i> EC ₅₀ (μM (SD ^a))	logD ^b	Kinetic solubility (μM) ^b	Rat S9 metabolic stability ^d	Human S9 metabolic stability ^d
	R ¹	R ³					
42	Me	Me	0.2 (0.061)	2.35	33.50	81	96
43	Me	<i>i</i> Pr	3.3 (0.25)	3.10	118.10	60	79
44	<i>i</i> Pr	Me	1.67 (0.35)	3.00	121.00	4	32

^aStandard deviation. ^bThe standard log *D* assay runs on 1 M concentration range using 10 mM DMSO stock solutions measured at pH 7.4. ^cThe standard kinetic solubility assay runs on 200 mM concentration range using 10 mM DMSO stock solutions. ^dLiver S9 metabolic stability assay at 3 μM, % remaining @ 60 min.

Scheme 2. Synthesis of Di(pyridin-2-yl)-1,3,4-thia-oxa-diazol-5-amine and Di(pyridin-2-yl)-1,2,4-triazol-5-amine^a

^aReagents and conditions: (a) SOCl₂, MeOH, 10–70 °C, 3 h, (b) N₂H₂, H₂O, MeOH, 70 °C, 92%, 10 h, (c) (III), DCM, 30 °C, 19 h, 16–38% (d) pTsOH, toluene, 100 °C, 6 h, 32–51%, (e) DMSO, EDCl, 60 °C, 2 h, 24–35%, or IBX, DCM, Et₃N, 0 °C, 1 h, 7%, (f) NH₄OH, DCM, 30 °C, 1 h, 53%, (g) MeI, CH₃CN, 40 °C, 16 h, 41%, (h) pyridine, 120 °C, 16 h, 10–29%.

this series of compounds. Compound 20 showed no improvement in metabolic stability; nevertheless, it did diminish the hERG activity (hERG IC₅₀ > 30 μM) likely resulting from reduction of the nitrogen pK_a.^{25,26} In general,

compounds in this series did not harbor a hERG concern (data in the Supporting Information). The combination of a CF₃ on either of the rings (A or B) with small alkyl substituents (R¹) on the A-ring provided the most potent compounds, albeit at a

Table 5. Pharmacokinetic Parameters for Selected Compounds in Various Species

analog	species	route	dose (mg/kg)	C_{max} (μ M)	T_{max} (h)	AUC _(0-inf) (μ M·h)	Cl (mL/min/kg)	V_{dss} (mL/kg)	%F	brain/plasma [b]/[p] ^a	efflux ratio (ER) ^b
1	mouse ^c	PO ^e	30	0.69 ± 0.18	0.5 ± 0.0	1.58 ± 0.27					
2	mouse ^c	PO ^e	30	1.26 ± 0.29	1.3 ± 0.5	3.61 ± 0.86					NC
10	mouse ^c	PO ^e	30	8.26 ± 2.6	1.0 ± 0.6	26.0 ± 9.0					1.4
19	mouse ^c	PO ^e	30	2.08 ± 1.22	0.5 ± 0.0	6.23 ± 6.16					0.9 ^k
31	mouse ^d	PO ^e	30	5.18	0.5	4.66 ± 0.54				1.10 (2 h)	1.0
	mouse ^e	PO ^e	10	0.65 ^h	0.5 ^h	0.94 ^h			13 ^h		
		IV ^f	2				62.9	3.01			
25	mouse ^c	PO ^e	30	2.05 ± 0.27	2.4 ± 3.8	20.0 ± 9.9					
32	mouse ^c	PO ^e	30	2.34 ± 0.52	0.5 ± 0.00	3.85 ± 0.76					
35	mouse ^c	PO ^e	30	0.21 ± 0.02	1.8 ± 1.7	1.73 ± 0.59					
47	mouse ^c	PO ^e	30	13.9 ^h	0.50 ^h	121 ^h				0.08 ^h	12
		PO ^g	10	5.27 ± 0.83	4.0 ± 2.8	68.1 ± NC ^j			57 ⁱ		
		IV ^f	2				3.6 ± 0.22	0.74 ± 0.08			

^aBrain to plasma ratio, based on AUC_{0-t}. ^bPermeability measured in a Madin Darby canine kidney cell, monolayer transfected with the multidrug resistance 1 (mdr1) gene encoding Pgp MDR1. ^cMale CD-1 ($n = 4$). ^dFemale BALB/c mouse. ^eAs a suspension CMC/Tween 0.5% methyl cellulose/0.25% Tween. ^f15% DMA/50% PEG400/35% D5W. ^gSuspension in 0.5% MC/0.25% Tween 80 in water. ^hData collected from non-serial sampling, no standard deviation reported. ⁱAUC extrapolation was above 23%. ^jNC = not calculated. ^kMeasured in Caco-2 cells.

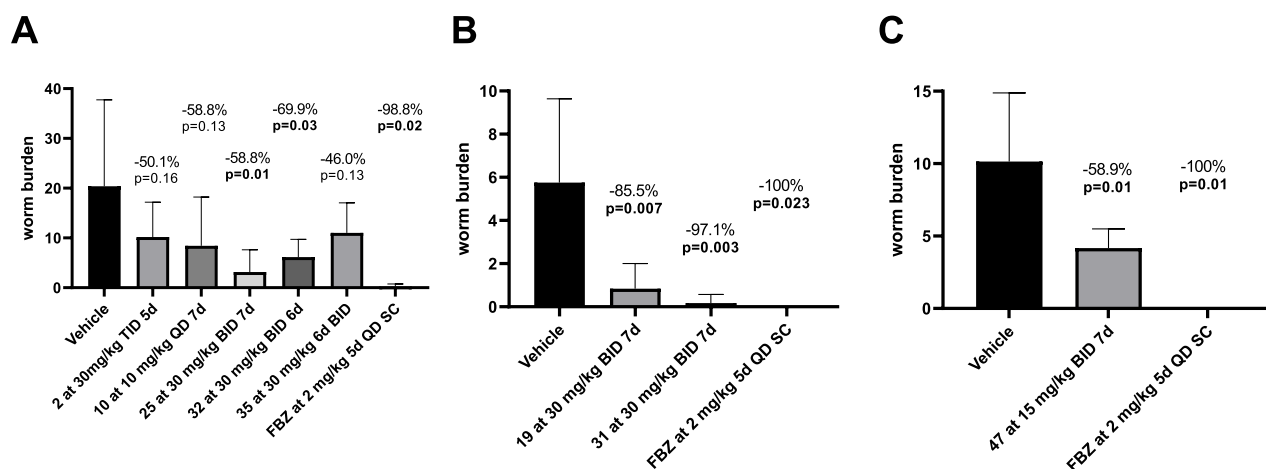


Figure 2. Adult worm burden in *L. sigmodontis*-infected female BALB/c mice and jirds after oral treatment with the candidates. Shown is the adult worm burden at 63–78 days after infection as mean plus standard deviation from the treatment groups and vehicle controls. (A) Mice have been naturally infected with *L. sigmodontis* for 35–37 days post infection and then treated orally. (B) Mice were subcutaneously infected with 40 infective L3 *L. sigmodontis* larvae and treated orally for 30–33 days post infection. (C) Jirds were subcutaneously infected with 40 infective L3 *L. sigmodontis* larvae and treated orally for 35–42 days post infection. Flubendazole (FBZ) was administered in all experiments subcutaneously (SC). Analysis was done using the unpaired two-tailed *t* test with $n = 5$ –8 animals per group; FBZ was given to three to four animals.

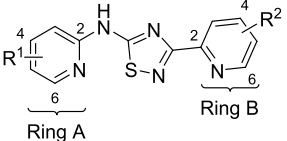
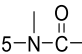
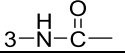
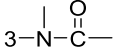
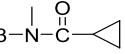
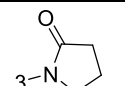
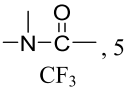
cost of aqueous solubility. Compounds such as 23, 24, 35, 37, and 38 (*O. gutturosa* EC₅₀ = 0.04, 0.05, 0.05, 0.05, and 0.02 μ M, respectively) showed aqueous solubilities <1 μ M or undetectable at the lowest measurable level. The ability to incorporate polarity on the A-ring did not necessarily impair activity and, in some instances, improved aqueous solubility. The 3-dimethyl amine as R¹ provided good microsomal stability while maintaining potency. It is interesting to note that no lipophilicity requirement for activity was observed for this series of compounds, and they resided in a good property space ($\log D_{7.4} < 4$) (Table 2). Ligand efficiency (LE, the measure of potency per atom) and ligand lipophilicity efficiency (LLE, the measure of potency relative to lipophilicity) were assessed to determine the relative efficiency for these compounds based on *O. gutturosa* *ex vivo* data generated for these series. Based on the evaluation of these parameters, the compounds emerged in desirable chemical space LE = 0.35–0.45 and LLE = 3–5, which are consistent

with optimized compounds (data in the Supporting Information).^{27,28} There also appeared to be no correlation of measured $\log D_{7.4}$ with metabolic stability; however, the general trend of increased lipophilicity resulting in poor solubility was observed.

Utilizing the preferred Me (R¹) and OiPr (R²) substituents, alternative six-membered N-containing heterocycles were evaluated on the 1,2,4-thiadiazole core (Table 3). Replacement of the A-ring with a pyrazine in 41 resulted in a ~8-fold increase in solubility when compared to the pyridine analog 10. Similarly, replacing the B-ring pyridyl with a pyrimidine (40) resulted in a ~4-fold improvement in solubility over 10 (Table 3) albeit resulting in a decrease in potency. The additional nitrogen in either A- or B-rings did not result in any improvement in activity or offer any additional improvements in microsomal stability.²⁹

Derivatization of the NH with small alkyl groups (R³) in compounds such as 43 and 44 did not abolish activity and

Table 6. *Ex Vivo O. gutturosa* Activity, Permeability, and Pgp Efflux

Analog			<i>O. gutturosa</i> EC ₅₀ μM (SD ^a)	logD ^b	Kinetic solubility (μM) ^c	Papp A-B (10 ⁻⁶ cm/s) ^d	Efflux ratio (ER) ^e	
	R ¹	R ²						
45	3-Me		11.90 (0.5)	1.70	2.35			
46		5- <i>OiPr</i>	1.27 (0.61)	2.40	29.45			
47			1.07 (0.50)	1.62	109.00	3.9	12.0	
48		4-CF ₃ , 5- <i>OiPr</i>	3.71 (0.50)	3.50	10.75	6.9	4.5	
49		4-CF ₃ , 5- <i>OiPr</i>	1.11 (0.35)	3.63	2.67	8.8	2.2	
50		5- <i>OiPr</i>	0.56 (0.50)	2.40	2.71	19.3	2.7	
51	3-Me, 5-N-C(=O)-	5- <i>OiPr</i>	0.49 (1.12)	2.20	15.00	30.3		
52		4-CF ₃ , 5- <i>OiPr</i>	1.73 (1.00)	2.70	9.95	12.9	3.9	
53		H	0.05 (0.43)	2.20	4.05			
54		5- <i>OiPr</i>	0.14 (0.35)	3.13	13.14	9.9	4.1	
55		4- <i>OiPr</i>	0.01 (0.25)	3.00	0.40	1.7	15.2	
56		4- <i>iPr</i>	0.01 (0.00)	3.10	5.60	3.2	8.4	
57		3-CO ₂ NMe ₂ , 5-CF ₃	5- <i>OiPr</i>	0.58 (0.00)	3.20	3.27		
58	3-CO ₂ NHMe	3- <i>OiPr</i>	0.62 (0.00)	2.15	130.20	11.2		
59		3-CO ₂ NH ₂	5- <i>OiPr</i>	2.66 (0.87)	1.60	0.30	0.8	4.6
60		3-CO ₂ NHMe		0.67 (0.87)	1.80	10.15		
61	3-CO ₂ NMe ₂		0.36 (1.06)	2.10	100.70	4.9	11.0	

^aStandard deviation. ^bThe standard log *D* assay runs on 1 M concentration range using 10 mM DMSO stock solutions measured at pH 7.4. ^cThe standard kinetic solubility assay runs on 200 mM concentration range using 10 mM DMSO stock solutions. ^dPermeability measured in a Madin Darby canine kidney cell, monolayer transfected with the multidrug resistance 1 (*mdr1*) gene encoding Pgp MDRI. ^eEfflux ratios (ER) are determined without and with valsopodar.

provided good solubility despite the increased log *D*_{7.4} (Table 4). The introduction of an R³ substituent likely disrupts planarity leading to improved aqueous solubility.³⁰

O. volvulus is the parasite responsible for onchocerciasis, and *ex vivo* testing against *O. volvulus* is only possible by recovering L3 infective larvae via the dissection of black flies and inducing *ex vivo* molting into L5 larvae.⁵ This is labor-intensive, low throughput, and not ideal for screening or lead optimization; therefore, only a limited subset of compounds could be tested. Some of the initial potent compounds against *O. gutturosa*, 11, 31, 32, 23, and 27, demonstrated 100% motility reduction of *O. volvulus* L5 larvae at 1 μM confirming antiparasitic activity against the human parasite and validating the series effectiveness at targeting the adult stage of the human disease, onchocerciasis (data in the Supporting Information).

At this point in the study, we chose to evaluate several potent compounds for *in vivo* pharmacokinetics and efficacy. When dosed orally at 30 mg/kg, select compounds had mouse plasma exposures that provided sufficient exposure and time above the EC₅₀ when dosed twice per day (BID) for efficacy evaluation *in vivo* (Table 5). Prioritization of compounds was based on *in vitro* potency and pharmacokinetic profile. These selected compounds were assessed in female BALB/c mice as oral BID regimens of 30 mg/kg for treatment times ranging from 1 to 7 days with the treatment starting at 30–37 days post infection (dpi), a time point at which adult worms had developed, and necropsies were performed at 63–78 dpi. Reduction of the adult *L. sigmodontis* worm burden was measured in comparison to the untreated/vehicle-treated control. In addition to the first thiazazole compound tested

in vivo (2, 30 mg/kg TID regimen for 5 days), a spread of efficacy was observed across the compounds tested (Figure 2). Compound 10, 30-fold more potent and with a 7-fold improved exposure, $AUC_{(0-inf)} = 26 \mu\text{M}\cdot\text{h}$, over 2 showed a 59% reduction of adult *L. sigmodontis* worms, when dosed at 10 mg/kg QD for 7 days. It should be noted that all compounds were tested in mice at a concentration of 30 mg/kg except for compound 10, which was dosed at a concentration of 10 mg/kg due to tolerability issues. Thus, even though compound 10 showed marked efficacy at a lower dose in comparison to the other compounds, further *in vivo* analysis was not pursued.

Compound 19, containing a basic nitrogen, demonstrated 86% reduction of adult worm burden at 30 mg/kg given BID for 7 days. Unfortunately, 19 contained a hERG liability (hERG $IC_{50} = 3.46 \mu\text{M}$) and would not progress any further. Compound 35, although potent (*O. gutturosa* $EC_{50} = 0.05 \mu\text{M}$), showed marginal reduction of adult worm burden (46%) at 30 mg/kg given BID for 6 days, which could be indicative of the poor exposure and poor solubility associated with the compound ($AUC_{(0-inf)} = 1.7 \mu\text{M}\cdot\text{h}$). Compound 25 showed reduction of adult worm burden (59%) given at 30 mg/kg BID for 7 days, which could be attributed to the compound's $AUC_{(0-inf)} = 20 \mu\text{M}\cdot\text{h}$ and perhaps the delayed T_{max} (2.4 h) relative to the other analogs ($T_{max} = 0.5 \text{ h}$), providing a more sustained coverage. Containing polar functionality as R^1 of the A-ring, compounds 31 and 32 demonstrated remarkable reduction of adult worm burden at 30 mg/kg BID, 97% reduction with compound 31 with 6 days of dosing and 70% reduction with compound 32 with 7 days of dosing. Subsequently, 31 was evaluated in chronically *L. sigmodontis*-infected microfilariae-positive jirds, confirming macrofilaricidal efficacy (71% reduction when dosed at 2.5 mg/kg SC for 7 days QD, data in the Supporting Information). The *in vivo* efficacy of compounds 31 and 32 appears to be driven by C_{max} as both compounds have a relatively modest pharmacokinetic profile in rodents. From the compounds tested *in vivo*, it appeared that analogs containing an ether, preferably the OiPr (R^2) substituent in the 5-position and the methyl or di-methyl amine (R^1) substituents in the 3-position, trended toward *in vivo* efficacy.

Based on ADME (absorption, distribution, metabolism, and excretion), physicochemical properties, and observed efficacy, 31 emerged as one of the most attractive compounds exhibiting acceptable plasma clearance and a low volume of distribution (V_{ss}) across multiple species (Supporting Information). Showing no *in vitro* safety concerns (Table 7), it was progressed into *in vivo* safety evaluation studies. During exploratory toxicological evaluation, CNS (central nervous system)-related observations were noted, and it was determined to halt further development of 31. It was shown that 31 crosses the blood brain barrier (BBB) efficiently (brain to plasma ratio: 1.1 (at 2 h)); hence, we focused efforts on compounds that would not cross the BBB, thereby limiting brain exposure. Since the mechanism of action of this series of compounds is not known, the best approach was to design analogs that would limit exposure within the brain.

Our approach was to target compounds with efflux ratio (ER) >2.5 in the MDCK cell line transfected with MDR1 (multidrug resistance-1 transfected Madin Darby canine kidney cell line). This MDCK/MDR1 cell line has been shown to identify compounds that are likely to be substrates for P-glycoprotein 1 (Pgp) and are unlikely to cross the BBB as an ER >2.5 is consistent with a brain to plasma ratio $[b]/[p]$ of

<0.2 and limited brain exposure.^{31,32} It is suggested that Pgp efflux is much greater in compounds containing more than two to three hydrogen bond donors (HBDs).^{33,34} Our goal was to impart structural elements designed to impart Pgp recognition.

Screening in the MDCK/MDR1 cell line identified compounds that had Pgp substrate potential, indicated by the high efflux ratio (Table 6). Compound 47, containing a methyl acetamide at the 3-position (R^1), was rapidly identified with a high efflux ratio of 12 while maintaining good permeability, $P_{appA-B} = 3.9 \times 10^{-6} \text{ cm/s}$, and consequently, 47 showed a brain to plasma ratio of 0.08, suggesting limited brain exposure (Table 5).

We focused new analogs on increasing polarity to limit brain exposure (Table 6). Cyclizing the acetamide (R^1) (52) resulted in good permeability and solubility with an ER = 3.9, whereas the introduction of the nitrogen-linked acetamide (R^2) on the B-ring (45) resulted in complete loss of activity. Exchanging the methyl on acetamide increased activity (50), although the small increase in lipophilicity resulted in decreased aqueous solubility and decreased efflux ratio (ER = 2.7). Compound 50 with ER = 2.7 and $P_{appA-B} = 19.3 \times 10^{-6} \text{ cm/s}$ still exhibited limited brain exposure, $[b]/[p] = 0.11$.

Introduction of carbon-linked amides in the 3-position of R^1 showed a range of activity and solubility. The primary amide (59) had no detectable solubility, poor permeability ($P_{appA-B} = 0.79 \times 10^{-6} \text{ cm/s}$), and less activity (*O. gutturosa* $EC_{50} = 2.6 \mu\text{M}$), whereas a tertiary amide (61) had improved solubility (101 μM), potency (*O. gutturosa* $EC_{50} = 0.36 \mu\text{M}$), and permeability ($P_{appA-B} = 4.9 \times 10^{-6} \text{ cm/s}$ and ER = 11). Combinations of the methyl acetamide with CF_3 provided some of the most potent compounds, 56 (*O. gutturosa* $EC_{50} = 0.01 \mu\text{M}$) and 55 (*O. gutturosa* $EC_{50} = 0.01 \mu\text{M}$). Interestingly, both 56 and 55 contained OiPr (R^2) groups at the 4-position rather than the previously observed optimal 5-position. These compounds also had good permeability and efflux ratios suggesting limited brain penetration, 56 (ER = 8.4) and 55 (ER = 15). Disappointingly, 55 had an aqueous solubility of $<1 \mu\text{M}$. Addition of a CF_3 (R^2) with the 5-OiPr on the B-ring, 34, did not add any benefits over 47 and was 10-fold less soluble with ER = 4.5. The addition of an acetamide in the 5-position of an already 3-Me (R^1) substituted A-ring resulted in ~ 8 -fold improved solubility, 51 compared to 10. Most of the analogs within this chemical series shared nearly identical properties as the total counts of HBDs and total polar surface areas (TPSA) remain constant; therefore, the significant changes in their Pgp recognition, efflux ratios, and/or permeability observed imply that further analysis of factors such as H-bond strength and intermolecular H-bonding may be required.

Compounds 47 and 50 showed 100% reduction of *O. volvulus* L5 larvae motility and viability at 1 μM confirming both antiparasitic activity against the human parasite and effectiveness of these new analogs (data in the Supporting Information). Finally, compound 47 was tested in *L. sigmodontis*-infected jirds and showed a significant reduction of 59% when dosed at 15 mg/kg orally for 7 days BID (Figure 2C).

Having identified compounds with limited brain exposure, further profiling was needed to determine whether the inhibition of Pgp would be of consequence for further development. Compound 47 still maintained high permeability in the MDCK wild-type cell line treated with elacridar (a Pgp and BCRP inhibitor),³¹ 47 $P_{appA-B} = 30 \times 10^{-6} \text{ cm/s}$. Compound 47 still maintained good oral exposure having

slow plasma clearance in the mouse, 3.6 mL/min/kg. Overall, the brain-limiting analogs maintained the promising ADME and safety profile of the previous analog.

In vitro cytotoxicity of select compounds was tested in a “normal” proliferating transformed human liver epithelial (THLE-2) cell line.³⁵ Compounds were incubated in THLE-2 cells for 24 and 72 h, and adenosine triphosphate (ATP) levels were used as an indicator of cell viability. Compounds 47 and 31 (Table 7) did not exhibit significant cellular cytotoxicity (additional compounds in the Supporting Information).

Table 7. *In Vitro* Safety Properties

<i>in vitro</i> ADME and safety	31	47
Plasma Protein Binding % (h/r)	>99/>99	90.7/95
Cytochrome P450s IC ₅₀ (μM) (3A4, 1A2, 2D6, 2C9, 2C19, 2C8)	22, >30, >30, 5.5, 20, 7.1	>30, >30, 30, 5.7, 29, >30
THLE ^a (cytotoxicity) ATP LC ₅₀ (μM)	36	106
hERG binding ^b (μM)	11.4	>30
CEREP ^c receptor, ion channel, transporter panel (binding at 10 μM)	5/76 >70%	1/76 >50%
Kinase selectivity panel at 3 μM	0/259	0/259
AMES-II/mini-AMES ^{d,e} micronucleus ^f	negative	negative negative

^a“Normal” proliferating transformed human liver epithelial (THLE-2) cell line. ^bCloned hERG potassium channels (encoded by the KCNH2 gene and expressed in HEK293 cells). ^cSecondary pharmacology targets were screened in the Eurofins CEREP non-kinase panel. ^dKinase, selectivity was evaluated in Thermo Fisher Scientific’s SelectScreen™ panel. ^eNon-mutagenic TA98, TA100, TA1535, TA97, and WP2 *uvrA* strains either in the presence or absence of metabolic activation (S9 fraction). ^fTK6 cells, in the presence and absence of Aroclor 1254-induced rat liver S9 activation.

In line with developing potential drug candidates, compounds were examined for additional ADME and safety properties (Table 7). Although having moderate solubilities, compounds displayed high permeability and moderate to high binding to human plasma proteins. To address any potential off target activity and potential safety concerns, compounds were screened against a panel of 70 secondary pharmacology targets³⁶ and up to 259 kinases.³⁷ Although compounds 47 and 31 contain the amino pyridine motif, they did not inhibit any kinases.³⁸ Only a few targets were observed at 10 μM in the secondary pharmacology binding assay. Low inhibition of hERG was observed, and compounds did not inhibit CYP3A4 and were not mutagenic in an AMES test (Table 7).

CONCLUSIONS

The initially identified amino-thiazole compound (1) showed a significant reduction of adult *L. sigmodontis* worm burden and provided a basis for lead optimization efforts. Through several modifications, a series of substituted di(pyridin-2-yl)-1,2,4-thiadiazol-5-amine compounds were discovered having *O. gutturosa* EC₅₀ < 100 nM and 100% inhibition (1 μM) against the human parasite *O. volvulus* L5 stage larvae. The series of substituted di(pyridin-2-yl)-1,2,4-thiadiazol-5-amine compounds showed a trend of reducing overall adult worm burden in the *L. sigmodontis* mouse and jird infection model. Additionally, other cores (i.e., TRZ and other TDZ regioisomers) from this series demonstrated favorable physical chemical and pharmacokinetic properties and potencies, which warrant further exploration should resources become available. However, there appears to be a disconnect in the *ex vivo* and *in*

in vivo efficacy correlation (EVIVC) that can possibly be attributed to several discrepancies, such as the fact that the *L. sigmodontis* and *O. gutturosa* rodent model used for screening are surrogate filarial nematodes to model human filarial diseases. While *O. gutturosa* is used as the screening surrogate of *O. volvulus*, this series of compounds has demonstrated activity against the *L. sigmodontis* parasite.²³ Last, the location of the parasite (thoracic cavity for *L. sigmodontis* versus subcutaneous and deep nodules for *O. volvulus*) might be of some consequence with regard to compound tissue distribution in this model.

Overall, this series of compounds maintains good ADME and physiochemical properties and these compounds are considered to be BCS Class II (good to high permeability yet poor solubility).³⁹ The brain-limiting compound 47 demonstrated efficacy in reducing adult worm burden in the jird *L. sigmodontis* infection model (Figure 2C), confirming macrofilaricidal efficacy.⁴⁰ To date, it is not clear which preclinical model predicts clinical efficacy nor adverse reactions related to the death of filarial parasites. In the future, clinical trials should be used to back translate efficacy in filarial preclinical models. However, based on our observation that adult worm clearance takes several weeks, we do not anticipate severe adverse events.

EXPERIMENTAL SECTION

***O. gutturosa* Adult Worm *Ex Vivo* Assay.** Activity against *O. gutturosa* adult male worms was determined using reported procedures.⁷ The EC₅₀ values were calculated using Microsoft Office Excel (2010) data analysis software. The tested compound is considered active when a motility reduction of ≥50% is observed by comparison to the untreated controls. *O. gutturosa* adult male worms were obtained postmortem from freshly slaughtered cattle. The worms were dissected from the nuchal ligament connective tissues of naturally infected cattle in Gambia, West Africa; the material was purchased from the International Trypanotolerance Centre, Banjul, from local butchers for use in this study. The adult worms were transferred individually to each well of a sterile 24-well (2 mL) plate (Thermo Fisher Scientific, UK) and maintained for at least 24 h in culture before use. The medium used was a minimum essential medium (MEM) with Earl’s salts and L-glutamine (Life Technologies Ltd., UK) supplemented with 10% heat inactivated newborn calf serum (Life Technologies Ltd., UK), 200 units/mL penicillin, 200 μg/mL streptomycin, and 0.5 μg/mL amphotericin B (Life Technologies Ltd., UK). Only normally active worms were used for the test, and all assays were conducted at 37 °C and 5% CO₂. The positive control drug used was Immiticide (melsarsomine dihydrochloride, Merial, USA). Known amounts of compounds were solubilized in 1 mL of DMSO. All stock solutions were allowed to stand at room temperature prior to use. The test items (four worms/drug concentration) were compared to untreated controls (six worms) and the positive control (two worms/drug concentration). Drug efficacy was assessed by the measurement of mean worm motility scores on a scale of 0 (immotile) to 10 (maximum) every 24 h, terminating at 120 h, using an Olympus inverted microscope. The results are reported as a percentage of the maximum score obtainable (100%) by calculating the motility index scores. The test drug is considered active when a motility reduction of ≥50% is observed by comparison to the untreated controls. The IC₅₀ value indicates the drug concentration that inhibited the motility by 50%. In addition, biochemical evaluation of worm viability was assessed using MTT/formazan colorimetry. The MTT assay was carried out after the last motility reading (120 h). Single intact worms were placed in each well of a 48-well plate (Thermo Fisher Scientific, UK) containing 0.5 mL of 0.5 mg/mL MTT (Sigma, UK) in PBS solution and then incubated for 30 min at 37 °C. The worms were removed, blotted carefully, and individually transferred to separate wells of a 96-well microtiter plate, each containing 200 μL of DMSO to solubilize the formazan. After 1

h, the plate was gently agitated to disperse the color evenly and the absorbance value (optical density, OD) of the resulting formazan solution was determined at 490 nm using an absorbance microplate reader (Biotek ELx800, Thermo Fisher Scientific, UK). The results are expressed as the mean OD per drug concentration. Inhibition of formazan formation is correlated with worm damage or death.

O. volvulus L5 Ex Vivo Assay. *O. volvulus* larvae (L4) were prepared using cryopreserved *O. volvulus* L3 cultured in a medium containing 1:1 NCTC-109 and IMDM (Iscove's modified Dulbecco's medium) supplemented with Glutamax (1×) and 2× Antibiotic-Antimycotic (Life Technologies). This culturing medium was then added in transwell 24-well plates containing human umbilical vein endothelial cell (HUVEC) monolayers, containing the L4 larvae. A week prior to conducting an assay, the cultured *O. volvulus* larvae (L5) were transferred into a Petri dish containing fresh medium. Aliquots of 8–10 worms were retrieved from the Petri dish and placed inside new transwells over newly seeded HUVEC monolayers in the medium described above. After the transfer of *O. volvulus* L5 to the plates, the test compounds were dissolved in DMSO, added to each well, and incubated at 37 °C in a 5% CO₂. The media containing freshly prepared compounds were partially replaced every 2–3 days for 14 days. After 14 days, the media were completely replaced. The untreated control contains the media described above with a final concentration of 0.05% DMSO. The motility was measured every 2–3 days with the following scale: 100% motility, constant coiling movement; 75% motility, slower coiling; 50% motility, slow and intermittent movement; 25% motility, very slow movement or twitching; and 0% motility, no movement. The motility was measured visually by two operators. On day 28, the viability of *O. volvulus* L5 was measured by MTT. Following washout and incubation during 1 h in PBS under 5% CO₂, worms were observed under an inverted microscope. Worms were considered dead if no staining or less than 50% within the worm was observed. Otherwise, if worms stained blue or more than 50% stained, then they are considered alive. All test treatments were performed in duplicates. Significance was determined using a *t* test.

Mouse Pharmacokinetics. All animal experiments were approved by the Institutional Animal Care and Use Committee (IACUC) of Bristol Myers Squibb. All studies were conducted in fed animals (male CD-1 mice) by Charles River Laboratories (Wilmington) Inc. Oral dosing (at specified doses, 10 mL/kg) was as a suspension in 0.5% carboxymethylcellulose, and 0.25% Tween 80 in water or in 0.5% methyl cellulose/0.25% Tween 80 in water and intravenous dosing (at specified doses) was a solution in 15% dimethylacetamide (DMA)/50% polyethylene glycol (PEG400)/35% DSW. Plasma samples (at 0.5, 1.5, 3, 5, and 8 h) were analyzed by LC–MS/MS, and the PK parameters were calculated using Phoenix WinNonlin software.

In Vivo Efficacy Using *L. sigmodontis*. All experimental procedures were performed in accordance with EU directive 2010/63/EU and the relevant national legislation, the “Décret no 2013–118, 1er février 2013, Ministère de l'Agriculture, de l'Agroalimentaire et de la Forêt”, national license number 75–1415. Animal protocols were approved by the ethical committee of the MNHN (Comité Cuvier, license: 68–002) and by the “Direction départementale de la cohésion sociale et de la protection des populations” (DDCSPP) (no. C75-05-15). The animal experiments done at IMMIP were approved by the Landesamt für Natur, Umwelt und Verbraucherschutz, Cologne, Germany (AZ 84-02.04.2015.A507). Female BALB/c mice (obtained from Janvier for IMMIP and Envigo for MNHN) were infected with *L. sigmodontis* at 6–8 weeks of age by natural exposure to the infected mite vector (IMMIP) or by subcutaneous injection of 40 infective L3 larvae (MNHN).⁷ Treatments were initiated at 30–37 days post-infection (dpi) in mice as previously described.⁷ Doses were given by oral gavage (10 mL/kg body weight) in milligrams of drug substance per kilograms of body weight of animals and are indicated in the Results and Discussion section and legend of Figure 2. Mice were sacrificed at 63–78 dpi. Female gerbils *Meriones unguiculatus* were infected at 6–8 weeks of age by natural infection via the mite vector at IMMIP or subcutaneously with 40 L3 larvae at the MNHN.

At the IMMIP, microfilariae-positive animals were subcutaneously treated once per day with compound 31 at 2.5 mg/kg for 7 days (*n* = 8). At the MNHN, jirds were treated after the development of adult worms for 30 days post infection. Treatment was done orally for 7 days BID with 15 mg/kg compound 47 (*n* = 6). Controls received vehicle treatments (*n* = 8). As positive control, gerbils and mice were subcutaneously treated with 2 mg/kg flubendazole for 5 days (*n* = 3–4). At the IMMIP, necropsies were performed 12 weeks after treatment started. The recovered *L. sigmodontis* adult worms were counted and analyzed by light microscopy to identify males and females. At the MNHN, necropsy was performed 70 days post infection. Differences in the protocols used between MNHN and IMMIP for the *L. sigmodontis* infection of jirds were caused by the COVID-19 restrictions in France that prevented long-term infections. Adult worm burden reduction was calculated by comparing the mean adult worm burden in vehicle controls to the adult worm burden in the treatment groups. Analysis was done using GraphPad Prism version 9.3.1 and an unpaired two-tailed *t* test with five to eight animals per group.

General. Compounds were named using ChemDraw Ultra 18.2. All materials were obtained from commercial sources and used without further purification unless otherwise noted. All air-sensitive reactions were carried out under a positive pressure of an inert nitrogen atmosphere. The reactions were monitored by thin-layer chromatography (TLC) carried out on silica gel plates (0.25 mm thick, GF254), and visualization was achieved by UV light. ¹H NMR (proton nuclear magnetic resonance) spectra and low-resolution electrospray ionization–MS (ESI–MS) were used for characterization. ¹H NMR spectra were measured on a Bruker or Varian 400 MHz spectrometer, and chemical shifts were reported in parts per million (δ , ppm) relative to the internal reference tetramethylsilane (Me₄Si). NMR spectra were acquired in CDCl₃, CD₃OD, or DMSO-*d*₆. ¹H NMR data are reported as follows: chemical shift [multiplicity (*s* = singlet, *d* = doublet, *t* = triplet, *q* = quartet, *dd* = doublet of doublets, *m* = multiplet, *brs* = broad singlet), *J* = coupling constant(s) (Hz), integration]. Low-resolution ESI–MS data were recorded on a Shimadzu LCMS-2020 mass spectrometer using an ESI source. LCMS conditions were included but not limited to the two as follows: Shimadzu LCMS-2020, Kinetex @ 5 μ m EVO C18 30 \times 2.1 mm, 5–95% MECN (0.01875% TFA) in water (0.0375% TFA), 1.5 min run, flow rate, 1.5 mL/min, UV detection (λ = 220 and 254 nm) or Shimadzu LCMS-2020, Kinetex EVO C18 2.1 \times 30mm, 5 μ m, 5–95% MECN in water (0.025% NH₃·H₂O), 1.5 min run, flow rate, 1.5 mL/min, UV detection (λ = 220, 254 nm). All the final compounds were purified to >95% purity. Conditions were as follows: Agilent 1200 LC and Agilent 6110 MSD, Phenomenex Gemini 3 μ m NX-C18, 4.6 \times 50 mm, 0–100%, A: 95% H₂O + 5% ACN (0.1% FA), B: 5% H₂O + 95% ACN (0.1% FA), 6 min run, flow rate, 1.0 mL/min, UV detection (λ = 214, 254 nm). Flash column chromatography was carried out using prepacked silica cartridges (from 4 up to 120 g) from Agela and eluted using a Biotage Companion system. All final compounds were purified to have purity higher than 95% by reverse-phase high-performance liquid chromatography (HPLC), normal phase flash chromatography, or crystallization. Reported yields were unoptimized. Calculations were carried out and plotted using Dotmatics Vortex v2016.10.56814.

General Procedure A for the Synthesis of Compounds in Tables 1–3 and 6. 3-(5-Isopropoxyppyridin-2-yl)-N-(3-methylpyridin-2-yl)-1,2,4-thiadiazol-5-amine (10). 5-Isopropoxypicolinonitrile. To a solution of propan-2-ol (1.18 g, 19.7 mmol, 1.49 mL) in *N,N*-dimethylformamide (40 mL) was added sodium hydride (983 mg, 24.6 mmol, 60% purity) at 0 °C under nitrogen. The mixture was stirred at 25 °C for 30 min, and 5-fluoropicolinonitrile (2.00 g, 16.4 mmol) was added to the reaction mixture at 0 °C under nitrogen. The mixture was stirred at 25 °C for 4 h and then poured into ice water. The aqueous phase was extracted with EtOAc, and the organic layers were washed with brine, dried over sodium sulfate, filtered, and concentrated to give a residue. The residue was purified by column chromatography to give 5-isopropoxypicolinonitrile (2.10 g, crude).

5-Isopropoxy-picolinimidamide. To a solution of 5-isopropoxy-picolinonitrile (500 mg, 3.08 mmol) in methanol (25 mL) was added sodium methanolate (16.6 mg, 308 μ mol), and the mixture was stirred at 25 °C for 8 h. Ammonium chloride (330 mg, 6.16 mmol) was added to the mixture and heated at 70 °C for 4 h. The mixture was concentrated under reduced pressure to give a residue, which was triturated with DCM (30 mL). The mixture was filtered, and the filter cake was dried to remove the solvent to give 5-isopropoxy-picolinimidamide hydrochloride (800 mg, crude, HCl).

2-Isothiocyanato-3-methylpyridine. To a solution of thiophosgene (5.32 g, 46.2 mmol) in DCM (80 mL) was added a solution of 3-methylpyridin-2-amine (5 g, 46.2 mmol) in DCM (50 mL) at -5 °C under a nitrogen atmosphere. The mixture was stirred at 25 °C for 3 h, and saturated sodium bicarbonate was added to the mixture. The mixture was extracted with DCM, and the combined organic layers were dried over sodium sulfate, filtered, and concentrated under reduced pressure to give a residue. The residue was purified by silica gel column chromatography to give 2-isothiocyanato-3-methylpyridine (1.00 g, 6.66 mmol, 14% yield).

5-Isopropoxy-N-((3-methylpyridin-2-yl)carbamothioyl)-picolinimidamide. To a solution of 2-isothiocyanato-3-methylpyridine (557 mg, 3.71 mmol) and Et₃N (3.75 g, 37.1 mmol, 5.14 mL) in DCM (15 mL) and acetone (15 mL) was added 5-isopropoxy-picolinimidamide hydrochloride (800 mg, 3.71 mmol, HCl). The mixture was stirred at 25 °C for 20 h, and then, the reaction mixture was concentrated under reduced pressure, diluted with water, and extracted with EtOAc. The combined organic layers were washed with brine, dried over sodium sulfate, filtered, and concentrated under reduced pressure to give 5-isopropoxy-N-((3-methylpyridin-2-yl)carbamothioyl)-picolinimidamide (350 mg, crude).

3-(5-Isopropoxy-pyridin-2-yl)-N-(3-methylpyridin-2-yl)-1,2,4-thiadiazol-5-amine. To a solution of 5-isopropoxy-N-((3-methylpyridin-2-yl)carbamothioyl)picolinimidamide (350 mg, 1.06 mmol) in THF (10 mL) was added diisopropyl azodicarbonate (DIAD) (279 mg, 1.38 mmol). The mixture was stirred at 25 °C for 20 h. The product was isolated and purified via standard methods to give 3-(5-isopropoxy-pyridin-2-yl)-N-(3-methylpyridin-2-yl)-1,2,4-thiadiazol-5-amine (126 mg, 0.385 mmol, 36% yield, 99.3% purity). ¹H NMR (400 MHz, DMSO-*d*₆) δ 8.35–8.29 (m, 2H), 8.17 (d, *J* = 8.8 Hz, 1H), 7.67 (d, *J* = 7.4 Hz, 1H), 7.51 (dd, *J* = 8.8, *J* = 2.9 Hz, 1H), 7.03 (dd, *J* = 7.2, *J* = 5.1 Hz, 1H), 4.81–4.75 (m, 1H), 2.40 (s, 3H), 1.33–1.32 (m, 6H); MS (ESI): *m/z* 328.2 [M + 1]⁺.

N,3-Di((pyridin-2-yl)-1,2,4-thiadiazol-5-amine) (9) (100% Purity). ¹H NMR (400 MHz, DMSO-*d*₆) δ ppm 12.31–12.51 (m, 1 H), 8.65–8.79 (m, 1 H), 8.41–8.55 (m, 1 H), 8.15–8.28 (m, 1 H), 7.91–8.00 (m, 1 H), 7.81–7.90 (m, 1 H), 7.44–7.52 (m, 1 H), 7.14–7.21 (m, 1 H), 7.05–7.13 (m, 1 H); MS (ESI): *m/z* 256.1 [M + 1]⁺.

N,N-Dimethyl-2-(5-((3-methylpyridin-2-yl)amino)-1,2,4-thiadiazol-3-yl)isonicotinamide (11) (57% Yield, 99% Purity). ¹H NMR (400 MHz, DMSO-*d*₆) δ 11.86 (s, 1H), 8.77 (d, *J* = 4.9 Hz, 1H), 8.33 (d, *J* = 4.3 Hz, 1H), 8.19 (s, 1H), 7.69 (d, *J* = 7.3 Hz, 1H), 7.49 (dd, *J*₁ = 4.8, *J*₂ = 1.4 Hz, 1H), 7.05 (dd, *J*₁ = 7.2, *J*₂ = 5.1 Hz, 1H), 3.03 (s, 3H), 2.93 (s, 3H), 2.41 (s, 3H); MS (ESI): *m/z* 341.3 [M + 1]⁺.

N,N-Dimethyl-6-(5-((3-methylpyridin-2-yl)amino)-1,2,4-thiadiazol-3-yl)nicotinamide (18) (52% Yield, 99% Purity). ¹H NMR (400 MHz, DMSO-*d*₆) δ 11.92 (brs, 1H), 8.75 (d, *J* = 1.6 Hz, 1H), 8.36–8.25 (m, 2H), 8.01 (dd, *J*₁ = 8.0, *J*₂ = 2.1 Hz, 1H), 7.69 (d, *J* = 7.2 Hz, 1H), 7.05 (dd, *J*₁ = 7.2, *J*₂ = 5.0 Hz, 1H), 3.07–2.95 (m, 6H), 2.42 (s, 3H); MS (ESI): *m/z* 341.1 [M + 1]⁺.

3-(3-Methyl-2-pyridyl)-N-(5-pyrrolidin-1-yl-2-pyridyl)-1,2,4-thiadiazol-5-amine (21) (21% Yield, 97% Purity). ¹H NMR (400 MHz, CD₃OD) δ 8.47 (d, *J* = 3.9 Hz, 1H), 7.86–7.77 (m, 2H), 7.41 (dd, *J*₁ = 7.8, *J*₂ = 4.8 Hz, 1H), 7.16 (dd, *J*₁ = 8.9, *J*₂ = 2.9 Hz, 1H), 7.02 (d, *J* = 8.8 Hz, 1H), 3.35–3.32 (m, 4H), 2.55 (s, 3H), 2.11–2.01 (m, 4H); MS (ESI): *m/z* 339.1 [M + 1]⁺.

3-(4-Methylpyridin-2-yl)-N-(3-(trifluoromethyl)pyridin-2-yl)-1,2,4-thiadiazol-5-amine (26) (10% Yield, 99% Purity). ¹H NMR (400 MHz, DMSO + D₂O) δ 8.71 (d, *J* = 4.5 Hz, 1H), 8.54 (d, *J* = 4.9 Hz, 1H), 8.16 (d, *J* = 6.5 Hz, 1H), 8.09 (s, 1H), 7.32 (d, *J* = 4.4 Hz,

1H), 7.18 (d, *J* = 5.6 Hz, 1H), 2.41 (s, 3H); MS (ESI): *m/z* 338.1 [M + 1]⁺.

N-(3-Methoxy-2-pyridyl)-3-(4-methyl-2-pyridyl)-1,2,4-thiadiazol-5-amine (29) (27% Yield, 99% Purity). ¹H NMR (400 MHz, DMSO-*d*₆) δ 11.85 (s, 1H), 8.54–8.52 (m, 1H), 8.10–8.08 (m, 1H), 8.03 (d, *J* = 4.4 Hz, 1H), 7.48–7.47 (m, 1H), 7.35–7.33 (m, 1H), 7.10 (s, 1H), 3.92 (s, 3H), 2.43 (s, 3H); MS (ESI): *m/z* 300.1 [M + 1]⁺.

N-(5-((1-Methylpiperidin-4-yl)oxy)pyridin-2-yl)-3-(pyridin-2-yl)-1,2,4-thiadiazol-5-amine (36) (34% Yield, 99% Purity). ¹H NMR (400 MHz, CD₃OD): δ 8.68 (m, 1H), 8.32 (d, *J* = 7.6 Hz, 1H), 8.20 (d, *J* = 2.8 Hz, 1H), 7.95–7.99 (m, 1H), 7.48–7.54 (m, 2H), 7.10 (d, *J* = 8.8 Hz, 1H), 4.48 (brs, 1H), 2.84 (brs, 2H), 2.51 (brs, 2H), 2.40 (s, 3H), 2.05–2.10 (m, 2H), 1.85–1.95 (m, 2H). MS (ESI) *m/z* 369.2, 370.2 [M + 1, M + 2]⁺.

General Procedure B for Compounds in Tables 1–4 and 6. **3-(5-Cyclopropoxy-pyridin-2-yl)-N-(3-methylpyridin-2-yl)-1,2,4-thiadiazol-5-amine (11).** 5-Cyclopropoxy-N-((3-methylpyridin-2-yl)carbamothioyl)picolinimidamide. To a solution of 2-isothiocyanato-3-methylpyridine (527 mg, 3.51 mmol) and triethylamine (710 mg, 7.02 mmol) in acetone (15 mL) and DCM (15 mL) was added 5-cyclopropoxy-picolinimidamide hydrochloride (500 mg, 2.34 mmol, HCl). The mixture was stirred at 25 °C for 20 h. 2-Isothiocyanato-3-methylpyridine (351 mg, 2.34 mmol) was added to the reaction mixture. The mixture was stirred at 25 °C for 4 h and then diluted with water. The aqueous phase was extracted with DCM, and the combined organic layers were washed with brine, dried over anhydrous sodium sulfate, filtered, and concentrated under reduced pressure to give a residue. The residue was purified by silica gel chromatography to give 5-cyclopropoxy-N-((3-methylpyridin-2-yl)carbamothioyl)picolinimidamide (400 mg, 0.782 mmol, 33% yield, 64% purity).

3-(5-Cyclopropoxy-pyridin-2-yl)-N-(3-methylpyridin-2-yl)-1,2,4-thiadiazol-5-amine. To a solution of 5-cyclopropoxy-N-((3-methylpyridin-2-yl)carbamothioyl)picolinimidamide (400 mg, 0.782 mmol) in ethanol (10 mL) was added a solution of iodine (39.7 mg, 0.156 mmol) in ethanol (0.5 mL) and hydrogen peroxide (177 mg, 1.56 mmol, 30% purity). The mixture was stirred at 25 °C for 6 h. The mixture was quenched with saturated sodium sulfite, and the aqueous phase was extracted with EtOAc. The combined organic layers were washed with brine, dried over anhydrous sodium sulfate, filtered, and concentrated under reduced pressure to give a residue. The residue was triturated with acetonitrile (10 mL). The filter cake and the filtrate showed a similar purity. The filter cake and filtrate were combined to give the crude product. The crude product was purified by prep-HPLC (column: Phenomenex Synergi C18 150 × 25 × 10 μ m; mobile phase: [water (0.225% FA)-ACN]; B%: 40% 70%, 11 min) to give 3-(5-cyclopropoxy-pyridin-2-yl)-N-(3-methylpyridin-2-yl)-1,2,4-thiadiazol-5-amine (61.95 mg, 0.187 mmol, 24% yield, 98.2% purity). ¹H NMR (400 MHz, DMSO-*d*₆) δ 11.79 (s, 1H), 8.43 (d, *J* = 2.7 Hz, 1H), 8.31 (d, *J* = 4.4 Hz, 1H), 8.21 (d, *J* = 8.7 Hz, 1H), 7.70–7.63 (m, 2H), 7.06–7.01 (m, 1H), 4.05–4.02 (m, 1H), 2.40 (s, 3H), 0.89–0.82 (m, 2H), 0.78–0.71 (m, 2H); MS (ESI): *m/z* 326.1 [M + 1]⁺.

3-[5-[(2-Cyclopropyl-2-azaspiro[3.3]heptan-6-yl)oxy]-2-pyridyl]-N-(3-methyl-2-pyridyl)-1,2,4-thiadiazol-5-amine (12) (12% Yield, 100% Purity). ¹H NMR (400 MHz, DMSO-*d*₆) δ 11.79 (s, 1H), 8.31–8.30 (dd, *J*₁ = 5.2, *J*₂ = 1.2 Hz, 1H), 8.27 (d, *J* = 2.4 Hz, 1H), 8.18 (s, 1H), 8.17–8.14 (d, *J* = 9.6 Hz, 1H), 7.68 (d, *J* = 7.2 Hz, 1H), 7.40–7.38 (dd, *J*₁ = 1.2, *J*₂ = 8.4 Hz, 1H), 7.05–7.02 (dd, *J*₁ = 7.2, *J*₂ = 5.2 Hz, 1H), 4.78–4.74 (m, 2H), 3.28 (s, 2H), 3.20 (s, 2H), 2.69–2.64 (m, 2H), 2.40 (s, 3H), 2.19–2.14 (m, 2H), 1.81–1.79 (m, 2H), 0.30–0.27 (m, 2H), 0.19–0.17 (m, 2H); MS (ESI): *m/z* 421.2 [M + 1]⁺.

6-(5-((3-Methylpyridin-2-yl)amino)-1,2,4-thiadiazol-3-yl)-nicotinonitrile (13) (74% Yield, 96% Purity). ¹H NMR (400 MHz, DMSO-*d*₆) δ 11.97 (s, 1H), 9.14 (d, *J* = 1.7 Hz, 1H), 8.49–8.44 (m, 1H), 8.40–8.36 (m, 1H), 8.33 (d, *J* = 4.0 Hz, 1H), 7.70 (d, *J* = 7.3 Hz, 1H), 7.06 (dd, *J*₁ = 7.3, *J*₂ = 5.1 Hz, 1H), 2.41 (s, 3H); MS (ESI): *m/z* 295.1 [M + 1]⁺.

3-[5-[(1-Cyclopropyl-4-piperidyl)oxy]-2-pyridyl]-N-(3-methyl-2-pyridyl)-1,2,4-thiadiazol-5-amine (19) (17% Yield, 99% Purity). ¹H

NMR (400 MHz, DMSO- d_6) δ 11.77 (s, 1H), 8.36 (d, J = 2.8 Hz, 1H), 8.31 (d, J = 3.9 Hz, 1H), 8.17 (d, J = 8.7 Hz, 1H), 7.67 (d, J = 7.1 Hz, 1H), 7.56 (dd, J_1 = 8.8, J_2 = 2.9 Hz, 1H), 7.03 (dd, J_1 = 7.3, J_2 = 5.1 Hz, 1H), 4.59–4.54 (m, 1H), 2.87–2.77 (m, 2H), 2.47–2.37 (m, 5H), 2.01–1.89 (m, 2H), 1.68–1.56 (m, 3H), 0.46–0.38 (m, 2H), 0.34–0.26 (m, 2H); MS (ESI): m/z 409.2 [M + 1]⁺.

3-(5-((1-Cyclopropyl-3,3-difluoropiperidin-4-yl)oxy)pyridin-2-yl)-N-(3-methylpyridin-2-yl)-1,2,4-thiadiazol-5-amine (20) (45% Yield, 98% Purity). ¹H NMR (400 MHz, methanol- d_4) δ 8.42 (d, J = 2.8 Hz, 1H), 8.32–8.28 (m, 2H), 7.67–7.62 (m, 2H), 7.00 (dd, J_1 = 7.2, J_2 = 5.2 Hz, 1H), 4.85–4.80 (m, 1H), 3.32–3.30 (m, 1H), 2.92–2.89 (m, 2H), 2.73–2.68 (m, 1H), 2.43 (s, 3H), 2.09–2.03 (m, 2H), 1.86–1.84 (m, 1H), 0.57–0.45 (m, 4H); MS (ESI): m/z 445.2 [M + 1]⁺.

3-(5-Cyclopropoxy)pyridin-2-yl)-N-(3-isopropylpyridin-2-yl)-1,2,4-thiadiazol-5-amine (23) (19% Yield, 95% Purity, HCl). ¹H NMR (400 MHz, DMSO- d_6) δ 11.86 (s, 1H), 8.44 (d, J = 2.8 Hz, 1H), 8.33 (d, J = 3.6 Hz, 1H), 8.22 (d, J = 8.8 Hz, 1H), 7.78 (d, J = 7.2 Hz, 1H), 7.66 (dd, J_1 = 8.8 Hz, J_2 = 2.8 Hz, 1H), 7.10 (d, J = 4.8 Hz, 1H), 4.05–4.02 (m, 1H), 3.57–3.35 (m, 1H), 1.22–1.21 (m, 6H), 0.86–0.83 (m, 2H), 0.76–0.72 (m, 2H). MS (ESI): m/z 354.2 [M + 1]⁺.

3-(5-Isopropoxy-4-(trifluoromethyl)pyridin-2-yl)-N-(3-isopropylpyridin-2-yl)-1,2,4-thiadiazol-5-amine (24) (19% Yield, 99% Purity). ¹H NMR (400 MHz, DMSO- d_6) 11.88 (s, 1H), 8.82 (s, 1H), 8.39 (s, 1H), 8.33 (dd, J_1 = 4.9, J_2 = 1.5, 1H), 7.79 (dd, J_1 = 7.6, J_2 = 1.3, 1H), 7.12 (dd, J_1 = 7.5, J_2 = 5.0, 1H), 5.15–5.06 (m, 1H), 3.60–3.50 (m, 1H), 1.37 (d, J = 6.0 Hz, 6H), 1.22 (d, J = 6.7 Hz, 6H). MS (ESI) m/z 424.2 [M + 1]⁺.

3-(5-Isopropoxy-2-pyridyl)-N-(3-isopropyl-2-pyridyl)-1,2,4-thiadiazol-5-amine (25) (71% Yield, 97% Purity). ¹H NMR (400 MHz, DMSO- d_6) δ 8.89 (brs, 1H), 8.40 (d, J = 2.8 Hz, 1H), 8.33 (dd, J_1 = 5.0, J_2 = 1.5 Hz, 1H), 8.25 (d, J = 8.8 Hz, 1H), 7.61 (dd, J_1 = 7.6, J_2 = 1.1 Hz, 1H), 7.31–7.28 (m, 1H), 7.02 (dd, J_1 = 7.6, J_2 = 5.0 Hz, 1H), 4.72–4.63 (m, 1H), 3.01–2.91 (m, 1H), 1.41–1.34 (m, 12H); MS (ESI): m/z 356.2 [M + 1]⁺.

3-(5-Isopropoxy)pyridin-2-yl)-N-(3-methoxy)pyridin-2-yl)-1,2,4-thiadiazol-5-amine (28) (31% Yield, 99% Purity). ¹H NMR (400 MHz, DMSO- d_6) δ 11.78 (brs, 1H), 8.33 (d, J = 2.8 Hz, 1H), 8.17 (d, J = 8.4 Hz, 1H), 8.02 (dd, J_1 = 1.2 Hz, J_2 = 5.2 Hz, 1H), 7.52–7.47 (m, 2H), 7.08 (dd, J_1 = 5.2 Hz, J_2 = 8 Hz, 1H), 4.80–4.77 (m, 1H), 3.91 (s, 3H), 1.34–1.32 (m, 6H). MS (ESI): m/z 344.2 [M + 1]⁺.

N²-(3-(5-Isopropoxy)pyridin-2-yl)-1,2,4-thiadiazol-5-yl)-N₃,N₃-dimethylpyridine-2,3-diamine (31) (15% Yield, 96% Purity). ¹H NMR (400 MHz, CD₃OD) δ 8.35–8.26 (m, 2H), 8.15 (d, J = 4.9 Hz, 1H), 7.65–7.54 (m, 2H), 7.06 (dd, J_1 = 7.7, J_2 = 5.0 Hz, 1H), 4.83–4.73 (m, 1H), 2.78 (s, 6H), 1.40 (d, J = 6.0 Hz, 6H); MS (ESI): m/z 357.1 [M + 1]⁺.

3-(4-Isopropylpyridin-2-yl)-N-(4-(trifluoromethyl)pyridin-2-yl)-1,2,4-thiadiazol-5-amine (35) (17% Yield, 98% Purity) as Off-White Solid. ¹H NMR (400 MHz, DMSO- d_6) δ 12.5 (brs, 1H), 8.74 (d, J = 5.6 Hz, 1H), 8.60 (d, J = 4.8 Hz, 1H), 8.09 (s, 1H), 7.42–7.38 (m, 3H), 3.03–2.98 (m, 1H), 1.27 (s, 6H). MS (ESI): m/z 366.1 [M + 1]⁺.

3-(3-Cyclopropoxy)pyridin-2-yl)-N-(5-isopropyl-4-(trifluoromethyl)pyridin-2-yl)-1,2,4-thiadiazol-5-amine (38) (13% Yield, 97% Purity). ¹H NMR (400 MHz, CDCl₃) δ 12.18 (s, 1H), 8.62 (s, 1H), 8.26 (dd, J_1 = 4.4, J_2 = 1.2 Hz, 1H), 7.67 (dd, J_1 = 8.4, J_2 = 1.2 Hz, 1H), 7.32 (dd, J_1 = 8.4, J_2 = 4.8 Hz, 1H), 6.82 (s, 1H), 3.72–3.58 (m, 1H), 3.27–3.20 (m, 1H), 1.34 (d, J = 6.8 Hz, 6H), 0.76–0.65 (m, 4H); MS (ESI) m/z 422.1 [M + 1]⁺.

3-(5-Isopropoxy)pyridin-2-yl)-N-(3-methyl-2-pyridyl)-1,2,4-thiadiazol-5-amine (39) (30% Yield, 92% Purity) as Yellow Solid. ¹H NMR (400 MHz, DMSO- d_6) δ 8.95 (s, 1H), 8.32 (s, 2H), 7.67 (d, J = 7.2 Hz, 1H), 7.04–7.01 (m, 1H), 5.36–5.30 (m, 1H), 2.40 (s, 3H), 1.36 (d, J = 6.0 Hz, 1H); MS (ESI): m/z 329.1 [M + 1]⁺.

3-(5-Isopropoxy)pyrimidin-2-yl)-N-(3-methylpyridin-2-yl)-1,2,4-thiadiazol-5-amine (40) (34% Yield, 98% Purity). ¹H NMR (400 MHz, DMSO- d_6) δ 11.89 (brs, 1H), 8.65 (s, 2H), 8.32 (dd, J = 0.9, 5.0 Hz, 1H), 7.68 (dd, J = 0.6, 7.3 Hz, 1H), 7.04 (dd, J = 5.0, 7.3 Hz, 1H), 4.98–4.86 (m, 1H), 2.40 (s, 3H), 1.35 (d, J = 6.0 Hz, 6H). MS (ESI): m/z 329.3 [M + 1]⁺.

3-(5-Isopropoxy-2-pyridyl)-N-(3-methylpyridin-2-yl)-1,2,4-thiadiazol-5-amine (41) (18% Yield, 96% Purity). ¹H NMR (400 MHz, DMSO- d_6) δ 12.22 (brs, 1H), 8.34 (d, J = 2.4 Hz, 2H), 8.21–8.15 (m, 2H), 7.52 (dd, J_1 = 8.8, J_2 = 2.9 Hz, 1H), 4.82–4.75 (m, 1H), 2.66 (s, 3H), 1.33 (d, J = 6.0 Hz, 6H); MS (ESI): m/z 329.1 [M + 1]⁺.

3-(5-Isopropoxy)pyridin-2-yl)-N-methyl-N-(3-methylpyridin-2-yl)-1,2,4-thiadiazol-5-amine (42) (13% Yield, 99% Purity). ¹H NMR (400 MHz, DMSO- d_6) δ 8.45–8.26 (m, 2H), 8.13 (d, J = 8.8 Hz, 1H), 7.83 (d, J = 7.2 Hz, 1H), 7.49 (dd, J_1 = 8.8, J_2 = 2.8 Hz, 1H), 7.27 (dd, J_1 = 7.6, J_2 = 4.8 Hz, 1H), 4.82–4.73 (m, 1H), 3.81 (s, 3H), 2.47 (s, 3H), 1.32 (d, J = 6.0 Hz, 6H); MS (ESI) m/z 342.2 [M + 1]⁺.

3-(5-Isopropoxy)pyridin-2-yl)-N-isopropyl-N-(3-methylpyridin-2-yl)-1,2,4-thiadiazol-5-amine (43) (54% Yield, 99% Purity Formic Acid). ¹H NMR (400 MHz, DMSO- d_6) δ 8.47 (d, J = 3.2 Hz, 1H), 8.31 (d, J = 2.8 Hz, 1H), 8.17 (s, 1H), 8.04 (d, J = 8.8 Hz, 1H), 7.48–7.45 (m, 2H), 4.79–4.73 (m, 1H), 4.57–4.52 (m, 1H), 2.27 (s, 3H), 1.37 (s, 3H), 1.35 (s, 3H), 1.32 (s, 3H), 1.30 (s, 3H); MS (ESI): m/z 370.1 [M + 1]⁺.

3-(5-Isopropoxy)pyridin-2-yl)-N-(3-isopropylpyridin-2-yl)-N-methyl-1,2,4-thiadiazol-5-amine (44) (55% Yield, 95% Purity). ¹H NMR (400 MHz, CD₃OD) 8.42 (dd, J_1 = 4.8, J_2 = 1.7 Hz, 1H), 8.27 (d, J = 2.6 Hz, 1H), 8.19 (d, J = 8.7 Hz, 1H), 8.06 (dd, J_1 = 7.9, J_2 = 1.7 Hz, 1H), 7.56–7.44 (m, 2H), 4.80–4.74 (m, 1H), 3.70 (s, 3H), 3.24–3.14 (m, 1H), 1.39 (d, J = 6.1 Hz, 6H), 1.30 (d, J = 6.8 Hz, 6H); MS (ESI) m/z 370.2 [M + 1]⁺.

N-(2-((3-(5-Isopropoxy)pyridin-2-yl)-1,2,4-thiadiazol-5-yl)amino)pyridin-3-yl)-N-methylacetamide (47) (70% Yield, 98% Purity). ¹H NMR (400 MHz, CDCl₃) 8.50 (d, J = 3.7 Hz, 1H), 8.39 (d, J = 2.4 Hz, 1H), 8.23 (d, J = 8.7 Hz, 1H), 7.58 (dd, J_1 = 7.6, J_2 = 1.2, 1H), 7.29 (dd, J_1 = 8.8, J_2 = 2.9, 1H), 7.13 (dd, J_1 = 7.6, J_2 = 5.0, 1H), 4.71–4.64 (m, 1H), 3.39 (s, 0.3H), 3.26 (s, 2.7H), 2.39 (s, 0.3H), 1.87 (s, 2.7H), 1.40 (d, J = 6.0 Hz, 6H); MS (ESI) m/z 385.2 [M + 1]⁺.

tert-Butyl Methyl(6-(5-((3-methylpyridin-2-yl)amino)-1,2,4-thiadiazol-3-yl)pyridin-3-yl)carbamate (45) (21% Yield, 99% Purity). ¹H NMR (400 MHz, DMSO- d_6) 11.84 (s, 1H), 8.69 (d, J = 2.1 Hz, 1H), 8.33 (d, J = 4.3 Hz, 1H), 8.28 (d, J = 8.3 Hz, 1H), 7.96 (d, J = 7.6 Hz, 1H), 7.68 (d, J = 7.2 Hz, 1H), 7.04 (dd, J_1 = 7.1, J_2 = 5.1 Hz, 1H), 3.29–3.22 (m, 3H), 2.41 (s, 3H), 1.94 (s, 3H); MS (ESI): m/z 341.2 [M + 1]⁺.

N-(2-((3-(5-Isopropoxy-4-(trifluoromethyl)pyridin-2-yl)-1,2,4-thiadiazol-5-yl)amino)pyridine-3-yl)-N-methylcyclopropanecarboxamide (49) (45% Yield, 99% Purity). ¹H NMR (400 MHz, DMSO- d_6) δ 12.85–12.04 (m, 1H), 8.81 (s, 1H), 8.50 (dd, J_1 = 4.9, J_2 = 1.3 Hz, 1H), 8.37 (s, 1H), 7.90 (d, J = 6.6 Hz, 1H), 7.26–7.12 (m, 1H), 5.16–5.07 (m, 1H), 3.45 (s, 0.4H), 3.12 (s, 2.5H), 1.37 (d, J = 6.0 Hz, 6H), 1.18–1.08 (m, 1H), 0.94–0.51 (m, 4H); MS (ESI): m/z 479.1 [M + 1]⁺.

N-(2-((3-(5-Isopropoxy)pyridin-2-yl)-1,2,4-thiadiazol-5-yl)amino)pyridin-3-yl)-N-methylcyclopropanecarboxamide (50) (98% Yield, 99% Purity). ¹H NMR (400 MHz, CDCl₃) δ 8.45–8.56 (m, 1H), 8.35–8.42 (m, 1H), 8.18–8.29 (m, 1H), 7.59–7.69 (m, 1H), 7.27–7.33 (m, 1H), 7.06–7.19 (m, 1H), 4.57–4.79 (m, 1H), 3.20–3.32 (m, 3H), 1.36–1.44 (m, 6H), 1.08–1.22 (m, 2H), 0.97–1.05 (m, 1H), 0.60–0.72 (m, 2H); MS(ESI): m/z 411.2 [M + 1]⁺.

1-(2-((3-(5-Isopropoxy-4-(trifluoromethyl)pyridin-2-yl)-1,2,4-thiadiazol-5-yl)amino)pyridin-3-yl)pyrrolidin-2-one (52) (32% Yield, 98% Purity). ¹H NMR (400 MHz, DMSO- d_6) δ 12.08 (s, 1H), 8.82 (s, 1H), 8.45 (dd, J_1 = 4.8 Hz, J_2 = 1.3 Hz, 1H), 8.38 (s, 1H), 7.85–7.83 (m, 1H), 7.21–7.18 (m, 1H), 5.15–5.08 (m, 1H), 3.74 (t, J = 7.0 Hz, 2H), 2.48–2.42 (m, 2H), 2.25–2.20 (m, 2H), 1.37 (s, 3H), 1.36 (s, 3H); MS (ESI): m/z 465.2 [M + 1]⁺.

N-(2-((3-(5-Isopropoxy)pyridin-2-yl)-1,2,4-thiadiazol-5-yl)amino)-5-(trifluoromethyl)pyridin-3-yl)-N-methylacetamide (54) (25% Yield, 99% Purity). ¹H NMR (400 MHz, DMSO- d_6) δ 13.00–12.51 (m, 1H), 8.91–8.83 (m, 1H), 8.38–8.32 (m, 1.5H), 8.18–8.16 (m, 1.5H), 7.52 (d, J_1 = 8.8, J_2 = 3.2 Hz, 1H), 4.81–4.76 (m, 1H), 3.31 (s, 1.9H), 3.10 (s, 1.3H), 2.22 (s, 1.6H), 1.73 (s, 1.4H), 1.32 (d, J = 6.0 Hz, 6H); MS (ESI): m/z 453.3 [M + 1]⁺.

N-(2-((3-(4-Isopropoxy)pyridin-2-yl)-1,2,4-thiadiazol-5-yl)amino)-5-(trifluoromethyl)pyridin-3-yl)-*N*-methylacetamide (**55**) (40% Yield, 95% Purity). ¹H NMR (400 MHz, DMSO-*d*₆) δ 13.13–12.68 (m, 1H), 8.97–8.88 (m, 1H), 8.59 (d, *J* = 6.3 Hz, 1H), 8.45–8.24 (m, 1H), 7.84 (dd, *J*₁ = 8.7, *J*₂ = 2.6 Hz, 1H), 7.34–7.32 (m, 1H), 5.02–4.94 (m, 1H), 3.32 (s, 1.6H), 3.11 (s, 1.4H), 2.23 (s, 1.6H), 1.74 (s, 1.4H), 1.38 (d, *J* = 6.0 Hz, 6H); MS (ESI): *m/z* 453.3 [M + 1]⁺.

N-(2-((3-(4-Isopropyl)pyridin-2-yl)-1,2,4-thiadiazol-5-yl)amino)-5-(trifluoromethyl)pyridin-3-yl)-*N*-ethylacetamide (**56**) (30% Yield, 96% Purity). ¹H NMR (400 MHz, DMSO-*d*₆) 13.14–12.48 (m, 1H), 8.95–8.83 (m, 1H), 8.58 (d, *J* = 5.0 Hz, 1H), 8.39 (s, 0.5H), 8.19 (d, *J* = 2.1 Hz, 0.5H), 8.13–8.12 (m, 1H), 7.39 (dd, *J* = 1.6, 5.0 Hz, 1H), 3.31 (s, 1.6H), 3.10 (s, 1.4H), 3.04–2.97 (m, 1H), 2.23 (s, 1.6H), 1.73 (s, 1.4H), 1.26 (d, *J* = 7.0 Hz, 6H), MS (ESI): *m/z* 437.3 [M + 1]⁺.

2-[[3-(3-Isopropoxy-2-pyridyl)-1,2,4-thiadiazol-5-yl]amino]-*N*,*N*-dimethyl-5-(trifluoromethyl)pyridine-3-carboxamide (**58**) (>100% Yield, 94% Purity). ¹H NMR (400 MHz, DMSO-*d*₆) δ = 12.65–12.29 (m, 1H), 8.94 (d, *J* = 1.1 Hz, 1H), 8.25–8.17 (m, 2H), 7.65 (d, *J* = 8.6 Hz, 1H), 7.47 (dd, *J*₁ = 4.5, *J*₂ = 8.4 Hz, 1H), 4.66–4.56 (m, 1H), 3.01 (s, 3H), 2.87 (s, 3H), 1.21 (d, *J* = 6.1 Hz, 6H). LCMS (ESI): *m/z* 453.1 [M + 1]⁺.

2-((3-(5-Isopropoxy)pyridin-2-yl)-1,2,4-thiadiazol-5-yl)amino)-nicotinamide (**59**) (55% Yield, 95% Purity). ¹H NMR (400 MHz, DMSO-*d*₆) 12.92 (s, 1H), 8.64 (dd, *J*₁ = 4.9, *J*₂ = 1.3 Hz, 1H), 8.60 (s, 1H), 8.45 (dd, *J*₁ = 7.8, *J*₂ = 1.5 Hz, 1H), 8.33 (d, *J* = 2.7 Hz, 1H), 8.17 (d, *J* = 8.8 Hz, 1H), 8.11 (s, 1H), 7.50 (dd, *J*₁ = 8.8, *J*₂ = 2.9 Hz, 1H), 7.25 (dd, *J*₁ = 7.8, *J*₂ = 5.0 Hz, 1H), 4.82–4.76 (m, 1H), 1.33 (d, *J* = 6.0 Hz, 6H); MS (ESI): *m/z* 357.3 [M + 1]⁺.

2-((3-(5-Isopropoxy)pyridin-2-yl)-1,2,4-thiadiazol-5-yl)amino)-*N*-methylnicotinamide (**60**) (69% Yield, 96% Purity). ¹H NMR (400 MHz, DMSO-*d*₆) 12.75 (s, 1H), 9.06 (s, 1H), 8.63 (d, *J* = 3.5 Hz, 1H), 8.41–8.28 (m, 2H), 8.18 (d, *J* = 8.8 Hz, 1H), 7.58–7.47 (m, 1H), 7.26–7.24 (m, 1H), 4.83–4.76 (m, 1H), 2.87 (d, *J* = 4.4 Hz, 3H), 1.33 (d, *J* = 6.1 Hz, 6H); MS (ESI): *m/z* 371.1 [M + 1]⁺.

2-((3-(5-Isopropoxy)pyridin-2-yl)-1,2,4-thiadiazol-5-yl)amino)-*N*,*N*-dimethylnicotinamide (**61**) (77% Yield, 99% Purity). ¹H NMR (400 MHz, DMSO-*d*₆) 11.91 (s, 1H), 8.52 (dd, *J*₁ = 5.0 Hz, *J*₂ = 1.6 Hz, 1H), 8.33 (d, *J* = 2.8 Hz, 1H), 8.16 (d, *J* = 8.7 Hz, 1H), 7.80 (dd, *J*₁ = 7.5 Hz, *J*₂ = 1.7 Hz, 1H), 7.52 (dd, *J*₁ = 8.7 Hz, *J*₂ = 2.9 Hz, 1H), 7.17 (dd, *J*₁ = 7.4 Hz, *J*₂ = 5.1 Hz, 1H), 4.83–4.73 (m, 1H), 3.02 (s, 3H), 2.88 (s, 3H), 1.32 (d, *J* = 6.0 Hz, 6H); MS (ESI): *m/z* 385.2 [M + 1]⁺.

Procedures for Compounds in Table 1 Containing Cores B, D, E, and F. 3-Methyl-*N*-[5-[5-(oxan-4-yloxy)pyridin-2-yl]-1,3,4-thiadiazol-2-yl]pyridin-2-amine (**4**). 5-(Tetrahydro-pyran-4-yloxy)pyridine-2-carboxylic Acid Hydrazide. To the stirred solution of 5-(tetrahydro-pyran-4-yloxy)-pyridine-2-carboxylic acid methyl ester (600 mg, 2.53 mmol) in methanol (10 mL), hydrazine hydrate (506 mg, 10.11 mmol) was added and the resulting mixture was heated at reflux for 2 h. After completion, the reaction mixture was concentrated under reduced pressure to provide 5-(tetrahydro-pyran-4-yloxy)-pyridine-2-carboxylic acid hydrazide (565 mg, 94% yield). MS (ESI): *m/z* 238.2 [M + 1]⁺.

N-[[3-(3-Methylpyridin-2-yl)carbamothioyl]amino]-5-(oxan-4-yloxy)pyridine-2-carboxamide. To a stirred solution of 5-(tetrahydro-pyran-4-yloxy)-pyridine-2-carboxylic acid hydrazide (500 mg, 2.17 mmol) in DCM (10 mL), 2-isothiocyanato-3-methyl-pyridine (379.8 mg, 2.53 mmol) was added and the reaction mixture was stirred at room temperature for 19 h. The reaction mixture was concentrated under reduced pressure to provide *N*-[[3-(3-methylpyridin-2-yl)carbamothioyl]amino]-5-(oxan-4-yloxy)pyridine-2-carboxamide (610 mg, 75% yield), which was used in the next step without further purification.

3-Methyl-*N*-[5-[5-(oxan-4-yloxy)pyridin-2-yl]-1,3,4-thiadiazol-2-yl]pyridin-2-amine. To a stirred solution of *N*-[[3-(3-methylpyridin-2-yl)carbamothioyl]amino]-5-(oxan-4-yloxy)pyridine-2-carboxamide (200 mg, 0.52 mmol) in toluene (5 mL), *p*-toluene sulfonic acid (98 mg, 0.57 mmol) was added at 25 °C and the resulting mixture was heated at 100 °C for 16 h. The reaction mixture was quenched with

water and extracted with 10% IPA-DCM. Combined organic layers were dried over anhydrous sodium sulfate, filtered, and evaporated under reduced pressure. The residue was purified by prep-HPLC to afford 3-methyl-*N*-[5-[5-(oxan-4-yloxy)pyridin-2-yl]-1,3,4-thiadiazol-2-yl]pyridin-2-amine (35 mg, 18% yield, 99% purity). ¹H NMR (400 MHz, DMSO-*d*₆): δ 10.86 (brs, 1H), 8.35 (d, *J* = 2.4 Hz, 1H), 8.21 (d, *J* = 4 Hz, 1H), 8.09 (d, *J* = 8.2 Hz, 1H), 7.62–7.57 (m, 2H), 6.69–6.93 (m, 1H), 4.75–4.71 (m, 1H), 3.86–3.83 (m, 2H), 3.50–3.45 (m, 2H), 2.34 (s, 3H), 2.01–1.98 (m, 2H), 1.65–1.57 (m, 2H); MS (ESI): *m/z* 370.2 [M + 1]⁺.

N-(3-Methylpyridin-2-yl)-3-((tetrahydro-2H-pyran-4-yl)oxy)pyridin-2-yl)-1,2,4-oxadiazol-5-amine (**6**). *N*-Hydroxy-5-((tetrahydro-2H-pyran-4-yl)oxy)picolinimidamide. To a solution of 5-((tetrahydro-2H-pyran-4-yl)oxy)picolinonitrile (1.50 g, 7.34 mmol) and triethylamine (2.23 g, 22.0 mmol) in ethanol (30.0 mL) was added hydroxylamine (510 mg, 7.34 mmol, HCl). The mixture was stirred at 80 °C for 16 h and then concentrated. The residue was diluted with 150 mL of ethyl acetate and 50 mL of brine. The organic phase was separated and dried over anhydrous sodium sulfate, filtered, and concentrated under vacuum to give *N*-hydroxy-5-((tetrahydro-2H-pyran-4-yl)oxy)picolinimidamide (1.60 g, crude).

3-(5-((Tetrahydro-2H-pyran-4-yl)oxy)pyridin-2-yl)-5-(trichloromethyl)-1,2,4-oxadiazole. To a solution of *N*-hydroxy-5-((tetrahydro-2H-pyran-4-yl)oxy)picolinimidamide (1.60 g, 6.74 mmol) in toluene (30 mL) was added trichloroacetic anhydride (4.16 g, 13.5 mmol). The mixture was stirred at 110 °C for 24 h. The mixture was concentrated and diluted with 100 mL of EtOAc. The organic phase was washed with saturated sodium bicarbonate and brine, dried over anhydrous sodium sulfate, filtered, and concentrated under vacuum. The residue was purified by column chromatography to give 3-(5-((tetrahydro-2H-pyran-4-yl)oxy)pyridin-2-yl)-5-(trichloromethyl)-1,2,4-oxadiazole (550 mg, 1.24 mmol, 18% yield, 82% purity). ¹H NMR (400 MHz, CDCl₃) δ 8.50 (d, *J* = 2.8 Hz, 1H), 8.11 (d, *J* = 8.8 Hz, 1H), 7.34 (dd, *J*₁ = 8.8, *J*₂ = 2.8 Hz, 1H), 4.70–4.61 (m, 1H), 4.05–3.97 (m, 2H), 3.66–3.60 (m, 2H), 2.13–2.02 (m, 2H), 1.90–1.81 (m, 2H).

3-Methylpyridin-2-yl)-[5-[5-(tetrahydro-pyran-4-yloxy)-pyridin-2-yl]-1,3,4]oxadiazol-2-yl]-amine (**7**). To a stirred solution of *N*-[[3-(3-methylpyridin-2-yl)carbamothioyl]amino]-5-(oxan-4-yloxy)-pyridine-2-carboxamide (400 mg, 1.03 mmol) in DCM (12 mL) was added triethylamine (0.3 mL, 2.06 mmol) and 2-iodoxybenzoic acid (IBX) (376.2 mg, 1.34 mmol) at 0 °C and stirred for 1 h under cooling conditions. Upon completion, the reaction mixture was diluted with DCM and washed with saturated NaHCO₃ solution, brine, dried over anhydrous sodium sulfate, filtered, and evaporated under reduced pressure. The residue was purified by repeated prep-TLC to provide the title compound (25 mg, 6.84% yield, 95.8% purity). ¹H NMR (400 MHz, DMSO-*d*₆): δ 13.26 (brs, 1H), 8.43 (s, 1H), 8.00 (d, *J* = 8.8 Hz, 1H), 7.96 (brs, 1H), 7.64–7.63 (m, 2H), 6.69 (m, 1H), 4.81–4.77 (m, 1H), 3.90–3.85 (m, 2H), 3.53–3.48 (m, 2H), 2.24 (s, 3H), 2.03–2.01 (m, 2H), 1.67–1.59 (m, 2H); MS (ESI): *m/z* 353.9 [M + 1]⁺.

3-Methyl-*N*-[5-[5-(oxan-4-yloxy)pyridin-2-yl]-4H-1,2,4-triazol-3-yl]pyridin-2-amine (**8**). 1-Benzoyl-3-(3-methylpyridin-2-yl)thiourea. To a stirred solution of 3-methylpyridin-2-amine (3.0 g, 27.14 mmol) in acetone (50 mL) was added benzoyl isothiocyanate (4.7 g, 28.85 mmol) at 0 °C and stirred for 1 h. The reaction mixture was warmed to room temperature and stirred for 2 h. The resultant solid was filtered, washed with cold water and Et₂O, and dried under vacuum to provide 1-benzoyl-3-(3-methylpyridin-2-yl)thiourea (3.2 g, 42% yield). MS (ESI): *m/z* 272.2 [M + 1]⁺.

3-Methylpyridin-2-yl)thiourea. A 10% aqueous NaOH solution (10 mL) was added to 1-benzoyl-3-(3-methylpyridin-2-yl)thiourea (3.2 g, 11.79 mmol) and heated to 80 °C for 40 min. The reaction mixture was cooled to 0 °C and acidified with 1(N) HCl to pH ~4. The mixture was then basified with saturated solution of KHCO₃ (pH ~8). The resulting solid was filtered, washed with cold water and Et₂O, and dried under vacuum to get (3-methylpyridin-2-yl)thiourea (1.8 g, 91% yield). MS (ESI): *m/z* 168.2 [M + 1]⁺.

N-(3-Methylpyridin-2-yl)(methylsulfanyl)methanimidamide. To a stirred solution of (3-methylpyridin-2-yl)thiourea (1.2 g, 7.17 mmol) in acetone (30 mL) was added MeI (4.5 mL, 71.76 mmol) at room temperature under an argon atmosphere. The resulting reaction mixture was stirred at RT for 18 h. The resulting solid was filtered, washed with acetone, and dried to afford the title compound (1.2 g, 92% yield). MS (ESI): m/z 182.3 $[M + 1]^+$.

3-Methyl-*N*-{5-[5-(oxan-4-yloxy)pyridin-2-yl]-4*H*-1,2,4-triazol-3-yl}pyridin-2-amine. To a stirred solution in a sealed tube was added 5-(oxan-4-yloxy)pyridine-2-carbohydrazide (450 mg, 1.89 mmol) in anhydrous pyridine (9 mL) *N*-(3-methylpyridin-2-yl)-(methylsulfanyl)methanimidamide (360 mg, 1.99 mmol) and heated to 140 °C for 5 h. The reaction mixture was concentrated under reduced pressure, and the residue was purified by column chromatography followed by trituration with 5% EtOAc ether to provide 3-methyl-*N*-{5-[5-(oxan-4-yloxy)pyridin-2-yl]-4*H*-1,2,4-triazol-3-yl}pyridin-2-amine (40 mg, 6% yield, 99% purity). ¹H NMR (400 MHz, DMSO-*d*₆): δ 13.37 (brs, 1H), 9.91 (s, 1H), 8.36 (s, 1H), 8.15 (s, 1H), 7.95 (d, J = 8.2 Hz, 1H), 7.54 (d, J = 6.8 Hz, 2H), 6.89 (m, 1H), 4.73–4.71 (m, 1H), 3.90–3.85 (m, 2H), 3.53–3.47 (m, 2H), 2.30 (s, 3H), 2.03–2.00 (m, 2H), 1.67–1.58 (m, 2H); MS (ESI): m/z 353.2 $[M + 1]^+$.

■ ASSOCIATED CONTENT

SI Supporting Information

The Supporting Information is available free of charge at <https://pubs.acs.org/doi/10.1021/acs.jmedchem.2c00960>.

Full experimental details for preparation of intermediates and compounds **1**, **5**, **14**, **15**, **17**, **22**, **27**, **30**, **32**, **34**, **37**, **43**, **46**, **48**, **51**, and **57** and NMR spectra and LCMS traces for key compounds; additional method details for log *D* and kinetic solubility measurement, metabolic stability, and permeability assays; molecular formula strings (SMILES); *O. gutturosa* motility and MTT viability inhibition EC₅₀, hERG IC₅₀, and *O. volvulus* L5 % inhibition; and MTT/formazan viability data and additional figures illustrating motility EC₅₀ curves and THLE-2 cytotoxicity data (PDF)

Excel file featuring the compounds used in this work (CSV)

■ AUTHOR INFORMATION

Corresponding Author

Natalie Hawryluk – Bristol Myers Squibb, San Diego, California 92121, United States; orcid.org/0000-0002-8930-1533; Email: nataliehawryluk@gmail.com

Authors

Dale Robinson – Bristol Myers Squibb, San Diego, California 92121, United States

Yixing Shen – Bristol Myers Squibb, San Diego, California 92121, United States

Graham Kyne – Zoetis, Kalamazoo, Michigan 49001, United States

Matthew Bedore – Zoetis, Kalamazoo, Michigan 49001, United States

Sanjay Menon – Zoetis, Kalamazoo, Michigan 49001, United States

Stacie Canan – Bristol Myers Squibb, San Diego, California 92121, United States

Thomas von Geldern – Embedded Consulting, Richmond, Illinois 60071, United States

Simon Townson – Northwick Park Institute for Medical Research, London HA1 3UJ, UK

Suzanne Gokool – Northwick Park Institute for Medical Research, London HA1 3UJ, UK

Alexandra Ehrens – Institute for Medical Microbiology, Immunology & Parasitology, University Hospital Bonn, 53127 Bonn, Germany; German Center for Infection Research (DZIF), 53127 Bonn, Germany

Marianne Koschel – Institute for Medical Microbiology, Immunology & Parasitology, University Hospital Bonn, 53127 Bonn, Germany

Nathaly Lhermitte-Vallarino – Unité Molécules de Communication et Adaptation des Microorganismes (MCAM, UMR 7245), Muséum national d'Histoire Naturelle, Paris 75005, France

Coralie Martin – Unité Molécules de Communication et Adaptation des Microorganismes (MCAM, UMR 7245), Muséum national d'Histoire Naturelle, Paris 75005, France

Achim Hoerauf – Institute for Medical Microbiology, Immunology & Parasitology, University Hospital Bonn, 53127 Bonn, Germany; German Center for Infection Research (DZIF), 53127 Bonn, Germany

Geraldine Hernandez – Bristol Myers Squibb, San Diego, California 92121, United States

Deepak Dalvie – Bristol Myers Squibb, San Diego, California 92121, United States

Sabine Specht – Institute for Medical Microbiology, Immunology & Parasitology, University Hospital Bonn, 53127 Bonn, Germany; Drugs for Neglected Diseases Initiative, Geneva 1204, Switzerland

Marc Peter Hübner – Institute for Medical Microbiology, Immunology & Parasitology, University Hospital Bonn, 53127 Bonn, Germany; German Center for Infection Research (DZIF), 53127 Bonn, Germany

Ivan Scandale – Drugs for Neglected Diseases Initiative, Geneva 1204, Switzerland

Complete contact information is available at:

<https://pubs.acs.org/doi/10.1021/acs.jmedchem.2c00960>

Notes

The authors declare the following competing financial interest(s): The contents are the responsibility of the Drugs for Neglected Diseases initiative and do not necessarily reflect the views of the donors. The funders had no role in the study design, data collection and analysis, decision to publish, or preparation of the manuscript. NAH, DR and SC are former employees of BMS, YS, GH and DD are employees of BMS. GK, MB and SM are employees of Zoetis. NAH, DR, SC, GH, and DD are BMS shareholders and GK, MB and SM are Zoetis shareholders with no other competing interest. All other authors have declared that no competing interests exist.

■ ACKNOWLEDGMENTS

We gratefully acknowledge the BMS San Diego DMPK, Toxicology, Formulations, and CLMD groups for their kind support. We especially acknowledge Joseph Piccotti, Kung-I Feng, and Cameron Reid for their excellent support of the project. We gratefully acknowledge Drs. Sara Lustigman and Nancy Tricoche for helpful discussions and for providing *O. volvulus* data. N.H. is grateful to Ken Duncan and Richard Elliot and the Bill & Melinda Gates Foundation for their generous support of the CGH macrofilaricide program. DNDi is grateful to the following donors for funding this project: Bill & Melinda Gates Foundation (#OPP1111431), USA and U.S.

Agency for International Development (USAID), USA; and to the donors contributing to DNDI's overall mission: UK aid, UK; Médecins sans Frontières (MSF); and the Swiss Agency for Development and Cooperation (SDC), Switzerland.

ABBREVIATIONS

ADME, absorption, distribution, metabolism, and excretion; ACN, acetonitrile; AT, aminothiazole; AUC, area under the plasma drug concentration time curve; BBB, blood brain barrier; CL, total clearance of drug from plasma; C_{max} , maximum plasma drug concentration during a dosing interval; DCM, dichloromethane; DMF, dimethylformamide; DMSO, dimethylsulfoxide; EtOAc, ethyl acetate; FA, formic acid; HOAc, glacial acetic acid; IPA, isopropyl alcohol; L5, young adult worms; dpi, days post infection; MDR1-MDCK, multidrug resistance-1 transfected Madin Darby canine kidney cell line; MeOH, methanol; MTT, 3-(4,5-dimethylthiazol-2-yl)-2,5-diphenyltetrazolium bromide; P_{app} , apparent permeability; PK, pharmacokinetic; PPB, plasma protein binding; *rac*, racemic; S9, supernatant from 9000 g × 20 min fractionation of liver preparation; THF, tetrahydrofuran; Vss, volume of distribution

REFERENCES

- (1) Cook, G. C.; Zumla, A., *Manson's Tropical Diseases*; Saunders: 2009.
- (2) Hawryluk, N. A.; Scandale, I. Onchocerciasis Drug Discovery. *Neglected Trop. Dis.: Drug Discovery Dev.* **2019**, *77*, 161–186.
- (3) Holmes, D. Loa loa: neglected neurology and nematodes. *Lancet Neurol.* **2013**, *12*, 631–632.
- (4) Hawryluk, N. A. Macrofilariocides: an unmet medical need for filarial diseases. *ACS Infect. Dis.* **2020**, *6*, 662–671.
- (5) Voronin, D.; Tricoche, N.; Jawahar, S.; Shlossman, M.; Bulman, C. A.; Fischer, C.; Suderman, M. T.; Sakanari, J. A.; Lustigman, S. Development of a preliminary in vitro drug screening assay based on a newly established culturing system for pre-adult fifth-stage *Onchocerca volvulus* worms. *PLoS Neglected Trop. Dis.* **2019**, *13*, No. e0007108.
- (6) Townson, S.; Ramirez, B.; Fakorede, F.; Mouries, M. A.; Nwaka, S. Challenges in drug discovery for novel antifilarials. *Expert Opin. Drug Discovery* **2007**, *2*, S63–S73.
- (7) Hübner, M. P.; Martin, C.; Specht, S.; Koschel, M.; Dubben, B.; Frohberger, S. J.; Ehrens, A.; Fendler, M.; Struever, D.; Mitre, E.; Vallarino-Lhermitte, N.; Gokool, S.; Lustigman, S.; Schneider, M.; Townson, S.; Hoerauf, A.; Scandale, I. Oxendazole mediates macrofilaricidal efficacy against the filarial nematode *Litomosoides sigmodontis* in vivo and inhibits *Onchocerca* spec. motility in vitro. *PLoS Neglected Trop. Dis.* **2020**, *14*, No. e0008427.
- (8) Jacobs, R. T.; Lunde, C. S.; Freund, Y. R.; Hernandez, V.; Li, X.; Xia, Y.; Carter, D. S.; Berry, P. W.; Halladay, J.; Rock, F.; Stefanakis, R.; Easom, E.; Plattner, J. J.; Ford, L.; Johnston, K. L.; Cook, D. A. N.; Clare, R.; Cassidy, A.; Myhill, L.; Tyrer, H.; Gamble, J.; Guimaraes, A. F.; Steven, A.; Lenz, F.; Ehrens, A.; Frohberger, S. J.; Koschel, M.; Hoerauf, A.; Hübner, M. P.; McNamara, C. W.; Bakowski, M. A.; Turner, J. D.; Taylor, M. J.; Ward, S. A. Boron-Pleuromutilins as anti-Wolbachia agents with potential for treatment of *Onchocerciasis* and lymphatic filariasis. *J. Med. Chem.* **2019**, *62*, 2521–2540.
- (9) Specht, S.; Pfarr, K. M.; Arriens, S.; Huebner, M. P.; Schulz, U. K.; Koschel, M.; Sternberg, S.; Martin, C.; Ford, L.; Taylor, M. J.; Hoerauf, A. Combinations of registered drugs reduce treatment times required to deplete *Wolbachia* in the *Litomosoides sigmodontis* mouse model. *PLoS Neglected Trop. Dis.* **2018**, *12*, e0006116/1–e0006116/20.
- (10) Schiefer, A.; Hübner, M. P.; Krome, A.; Lämmer, C.; Ehrens, A.; Aden, T.; Koschel, M.; Neufeld, H.; Chaverra-Muñoz, L.; Jansen, R.; Kehraus, S.; König, G. M.; Pogorevc, D.; Müller, R.; Stadler, M.; Hüttel, S.; Hesterkamp, T.; Wagner, K.; Pfarr, K.; Hoerauf, A. Corallopyronin A for short-course anti-wolbachial, macrofilaricidal treatment of filarial infections. *PLoS Neglected Trop. Dis.* **2020**, *14*, No. e0008930.
- (11) Ehrens, A.; Lunde, C. S.; Jacobs, R. T.; Struever, D.; Koschel, M.; Frohberger, S. J.; Lenz, F.; Fendler, M.; Turner, J. D.; Ward, S. A.; Taylor, M. J.; Freund, Y. R.; Stefanakis, R.; Easom, E.; Li, X.; Plattner, J. J.; Hoerauf, A.; Hübner, M. P. In vivo efficacy of the boron-pleuromutilin AN11251 against *Wolbachia* of the rodent filarial nematode *Litomosoides sigmodontis*. *PLoS Neglected Trop. Dis.* **2020**, *14*, No. e0007957.
- (12) Von Geldern, T. W.; Morton, H. E.; Clark, R. F.; Brown, B. S.; Johnston, K. L.; Ford, L.; Specht, S.; Carr, R. A.; Stolarik, D. F.; Ma, J.; Rieser, M. J.; Struever, D.; Frohberger, S. J.; Koschel, M.; Ehrens, A.; Turner, J. D.; Hübner, M. P.; Hoerauf, A.; Taylor, M. J.; Ward, S. A.; Marsh, K.; Kempf, D. J. Discovery of ABBV-4083, a novel analog of Tylosin A that has potent anti-Wolbachia and anti-filarial activity. *PLoS Neglected Trop. Dis.* **2019**, *13*, No. e0007159.
- (13) Hübner, M. P.; Koschel, M.; Struever, D.; Nikolov, V.; Frohberger, S. J.; Ehrens, A.; Fendler, M.; Johannes, I.; von Geldern, T. W.; Marsh, K.; Turner, J. D.; Taylor, M. J.; Ward, S. A.; Pfarr, K.; Kempf, D. J.; Hoerauf, A. In vivo kinetics of *Wolbachia* depletion by ABBV-4083 in *L. sigmodontis* adult worms and microfilariae. *PLoS Neglected Trop. Dis.* **2019**, *13*, No. e0007636.
- (14) Bakowski, M. A.; Shiroodi, R. K.; Liu, R.; Olejniczak, J.; Yang, B.; Gagaring, K.; Guo, H.; White, P. M.; Chappell, L.; Debec, A.; Landmann, F.; Dubben, B.; Lenz, F.; Struever, D.; Ehrens, A.; Frohberger, S. J.; Sjoberg, H.; Pionnier, N.; Murphy, E.; Archer, J.; Steven, A.; Chunda, V. C.; Fombad, F. F.; Chounna, P. W.; Njouendou, A. J.; Metuge, H. M.; Ndzeshang, B. L.; Gandjui, N. V.; Akumtuh, D. N.; Kwentu, T. D. B.; Woods, A. K.; Joseph, S. B.; Hull, M. V.; Xiong, W.; Kuhlen, K. L.; Taylor, M. J.; Wanji, S.; Turner, J. D.; Hübner, M. P.; Hoerauf, A.; Chatterjee, A. K.; Roland, J.; Tremblay, M. S.; Schultz, P. G.; Sullivan, W.; Chu, X.-J.; Petrassi, H. M.; McNamara, C. W. Discovery of short-course anti-wolbachial quinazolines for elimination of filarial worm infections. *Sci. Transl. Med.* **2019**, *11*, No. eaav3523.
- (15) Hawryluk, N.; Zhiru, L.; Carlow, C.; Gokool, S.; Townson, S.; Kreiss, T.; Chojnowski, A.; Prorok, M.; Siekierka, J.; Ehrens, A.; Koschel, M.; Lhermitte-Vallarino, N.; Martin, C.; Hoerauf, A.; Hernandez, G.; Canan, S.; Khetani, V.; Zeldis, J.; Specht, S.; Hübner, M. P.; Scandale, I. Filarial nematode phenotypic screening cascade to identify compounds with anti-parasitic activity for drug discovery optimization. *Int. J. Parasitol.: Drugs Drug Resist.* **2022**, *19*, 89–97.
- (16) Devine, S. M.; Mulcair, M. D.; Debono, C. O.; Leung, E. W. W.; Nissink, J. W. M.; Lim, S. S.; Chandrashekar, I. R.; Vazirani, M.; Mohanty, B.; Simpson, J. S.; Baell, J. B.; Scammells, P. J.; Norton, R. S.; Scanlon, M. J. Promiscuous 2-Aminothiazoles (PrATs): A frequent hitting scaffold. *J. Med. Chem.* **2015**, *58*, 1205–1214.
- (17) Blagg, J. Structure-activity relationships for in vitro and in vivo toxicity. *Annu. Rep. Med. Chem.* **2006**, *41*, 353–368.
- (18) Kalgutkar, A. S.; Gardner, I.; Obach, R. S.; Shaffer, C. L.; Callegari, E.; Henne, K. R.; Mutlib, A. E.; Dalvie, D. K.; Lee, J. S.; Nakai, Y.; O'Donnell, J. P.; Boer, J.; Harriman, S. P. A comprehensive listing of bioactivation pathways of organic functional groups. *Curr. Drug Metab.* **2005**, *6*, 161–225.
- (19) Kalgutkar, A. S.; Dalvie, D. Predicting toxicities of reactive metabolite-positive drug candidates. *Annu. Rev. Pharmacol. Toxicol.* **2015**, *55*, 35–54.
- (20) Yang, S.-J.; Lee, S.-H.; Kwak, H.-J.; Gong, Y.-D. Regioselective Synthesis of 2-Amino-Substituted 1,3,4-Oxadiazole and 1,3,4-Thiadiazole Derivatives via reagent-based cyclization of thiosemicarbazide intermediate. *J. Org. Chem.* **2013**, *78*, 438–444.
- (21) Chaudhari, P. S.; Pathare, S. P.; Akamanchi, K. G. o-Iodoxybenzoic Acid mediated oxidative desulfurization initiated domino reactions for synthesis of azoles. *J. Org. Chem.* **2012**, *77*, 3716–3723.

- (22) Dalvie, D. K.; Kalgutkar, A. S.; Khojasteh-Bakht, S. C.; Obach, R. S.; O'Donnell, J. P. Biotransformation reactions of five-membered aromatic heterocyclic Rings. *Chem. Res. Toxicol.* **2002**, *15*, 269–299.
- (23) Hawryluk, N.; Canan, S. S.; Condroski, K. R.; Kyne, G.; Bedore, M.; Menon, S. Heterocyclic compounds and their use for treatment of helminthic infections and diseases. WO2020219871A1, 2020.
- (24) Duffus, J. H.; Nordberg, M.; Templeton, D. M. Glossary of terms used in toxicology, 2nd edition (IUPAC Recommendations 2007). *Pure Appl. Chem.* **2007**, *79*, 1153–1344.
- (25) Meanwell, N. A. Fluorine and Fluorinated Motifs in the Design and Application of Bioisosteres for Drug Design. *J. Med. Chem.* **2018**, *61*, 5822–5880.
- (26) Pettersson, M.; Hou, X.; Kuhn, M.; Wager, T. T.; Kauffman, G. W.; Verhoest, P. R. Quantitative Assessment of the Impact of Fluorine Substitution on P-Glycoprotein (P-gp) Mediated Efflux, Permeability, Lipophilicity, and Metabolic Stability. *J. Med. Chem.* **2016**, *59*, 5284–5296.
- (27) Hopkins, A. L.; Keserü, G. M.; Leeson, P. D.; Rees, D. C.; Reynolds, C. H. The role of ligand efficiency metrics in drug discovery. *Nat. Rev. Drug Discovery* **2014**, *13*, 105–121.
- (28) Hopkins, A. L.; Groom, C. R.; Alex, A. Ligand efficiency: a useful metric for lead selection. *Drug Discovery Today* **2004**, *9*, 430–431.
- (29) St. Jean, D. J., Jr.; Fotsch, C. Mitigating heterocycle metabolism in drug discovery. *J. Med. Chem.* **2012**, *55*, 6002–6020.
- (30) Ishikawa, M.; Hashimoto, Y. Improvement in aqueous solubility in small molecule drug discovery programs by disruption of molecular planarity and symmetry. *J. Med. Chem.* **2011**, *54*, 1539–1554.
- (31) Rowbottom, C.; Pietrasiewicz, A.; Tuczewycz, T.; Grater, R.; Qiu, D.; Kapadnis, S.; Trapa, P. Optimization of dose and route of administration of the P-glycoprotein inhibitor, valsopodar (PSC-833) and the P-glycoprotein and breast cancer resistance protein dual-inhibitor, elacridar (GF120918) as dual infusion in rats. *Pharmacol. Res. Perspect.* **2021**, *9*, No. e00740.
- (32) Doan, K. M. M.; Humphreys, J. E.; Webster, L. O.; Wring, S. A.; Shampine, L. J.; Serabjit-Singh, C. J.; Adkison, K. K.; Polli, J. W. Passive Permeability and P-Glycoprotein-Mediated Efflux Differentiate Central Nervous System (CNS) and non-CNS marketed drugs. *J. Pharmacol. Exp. Ther.* **2002**, *303*, 1029.
- (33) Hitchcock, S. A. Structural modifications that alter the P-glycoprotein efflux properties of compounds. *J. Med. Chem.* **2012**, *55*, 4877–4895.
- (34) Desai, P. V.; Raub, T. J.; Blanco, M.-J. How hydrogen bonds impact P-glycoprotein transport and permeability. *Bioorg. Med. Chem. Lett.* **2012**, *22*, 6540–6548.
- (35) Benbow, J. W.; Aubrecht, J.; Banker, M. J.; Nettleton, D.; Aleo, M. D. Predicting safety toleration of pharmaceutical chemical leads: cytotoxicity correlations to exploratory toxicity studies. *Toxicol. Lett.* **2010**, *197*, 175–182.
- (36) Eurofins Cerep, Le Bois l'Évêque B.P. 30001, 86 600 Celle l'Évescault, France. Compound binding was calculated as a % inhibition of the binding of a radioactively labeled ligand specific for each target. Results showing an inhibition higher than 50% are considered to represent significant effects of the test compounds.
- (37) *Select Screen Kinase Profiling Services*; Life Technologies, Inc.: Madison WI, USA.
- (38) Xing, L.; Klug-Mcleod, J.; Rai, B.; Lunney, E. A. Kinase hinge binding scaffolds and their hydrogen bond patterns. *Bioorg. Med. Chem.* **2015**, *23*, 6520–6527.
- (39) Tsume, Y.; Mudie, D. M.; Langguth, P.; Amidon, G. E.; Amidon, G. L. The biopharmaceutics classification system: subclasses for in vivo predictive dissolution (IPD) methodology and IVIVC. *Eur. J. Pharm. Sci.* **2014**, *57*, 152–163.
- (40) Morris, C. P.; Evans, H.; Larsen, S. E.; Mitre, E. A. Comprehensive, model-based review of vaccine and repeat infection trials for filariasis. *Clin. Microbiol. Rev.* **2013**, *26*, 381.